L-PBF Material Process Record

Title: MP_BlueOrigin_ACO_M2_GRCop42	
Record Number: MP_BlueOrigin_ACO_M2_GRCop42	
General Description: Powder bed fusion GRCop42	
Approval Statement: This document was developed as part of an Advanced Collaboration Opportunity between NASA Marshall Space Flight Center (MSFC) and Blue Origin. It draws comparisons to MSFC GRCop-42 data and NASA-STD-6030 requirements. It should not, however, be interpreted as a complete qualification to NASA-STD-6030 requirements.	
CEO Review: Brian West	Date: 5/18/2022

L-PBF Metallurgical Process Definition

Powder Feedstock	
Feedstock Specification:	PAC GRCop42 Lot#: AMPGR42NASAAM21030
Reuse protocol:	No Reuse

Powder Specification and Certifications

Powder procured IAW *GRCop-42 Alloy Gas Atomized Powder Specification, Rev 1-29, issued 7/22/2020*

Powder CoC available upon request.

Fusion Process Controls			
Machine ID:	Concept Laser	Model/Model:	M2
Serial Number:	M2-2021-02-02	Configuration Date:	5/20/21 - 9/9/21
Slicer Software:	Materialize Magics	Software Version:	25.02
Recoater Configuration:	Steel Blade		
Build platform material:	Stainless steel, In 718 coating		
Preheat temperature:	None		
Nominal dosing range:	Variable		
Purge Gas composition:	Argon		
Argon gas flow:	60mm/s		
Oxygen limit:	Not directly controlled, but typically in ~0.01-0.05% range		
Humidity and Temperature controls:	Not measured/controlled		
Parameter File:	GRCop42_Material_Parameter	Hash:	N/A
Layer thickness:	30µm		
Other:	N/A		

Post Processing	Builds processed per this material process will receive the following thermal treatments: <u>Stress Relief</u> – 400C for 1 hour <u>HIP</u> – Standard MSFC HIP Profiles

Process Restart
Process restart not allowed, however several build stops escaped internal processes and restarts did occur in initial builds. Details of specific build stops and restarts are discussed in Appendix 1. Specific restart study under more controlled conditions is in work. Restart criteria and procedure: Not yet formally established.

Build Set Utilized: 2021-0221 Dimensional Analysis

Purpose: Determine if machine is consistent across the build plate, if not avoid areas in future builds.

Overall Layout

TOP

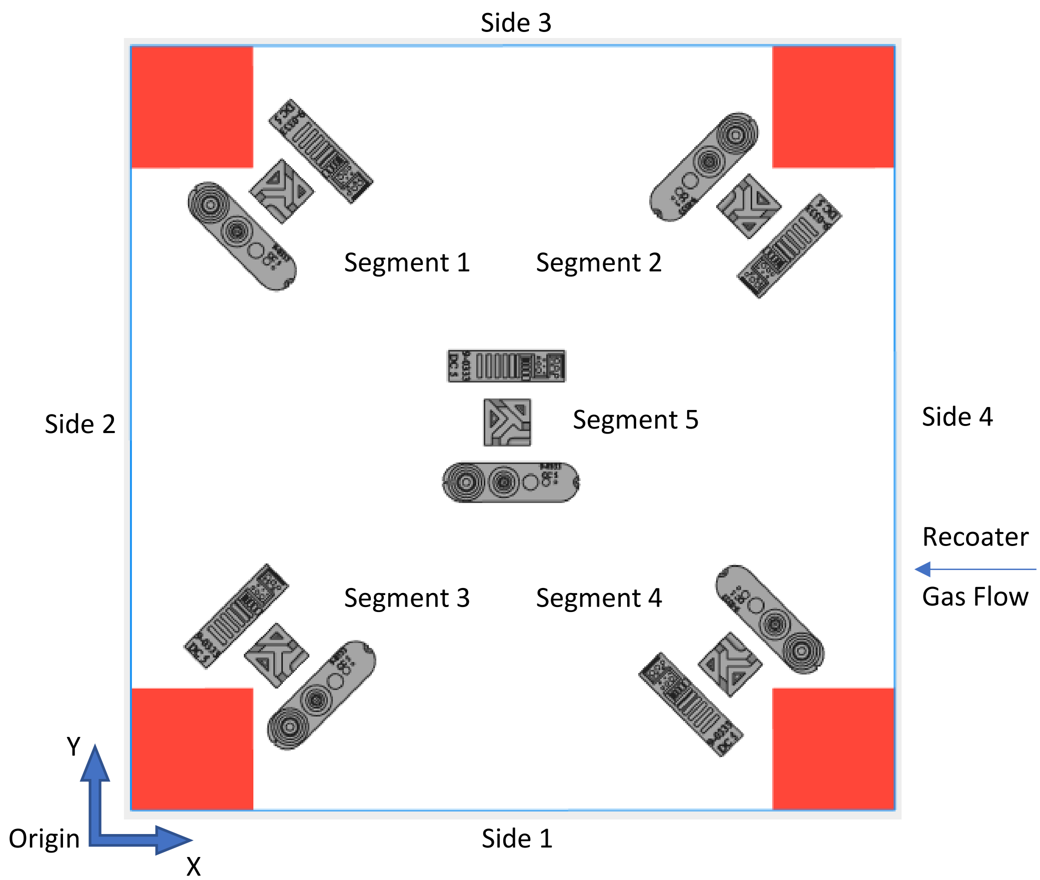

ISO

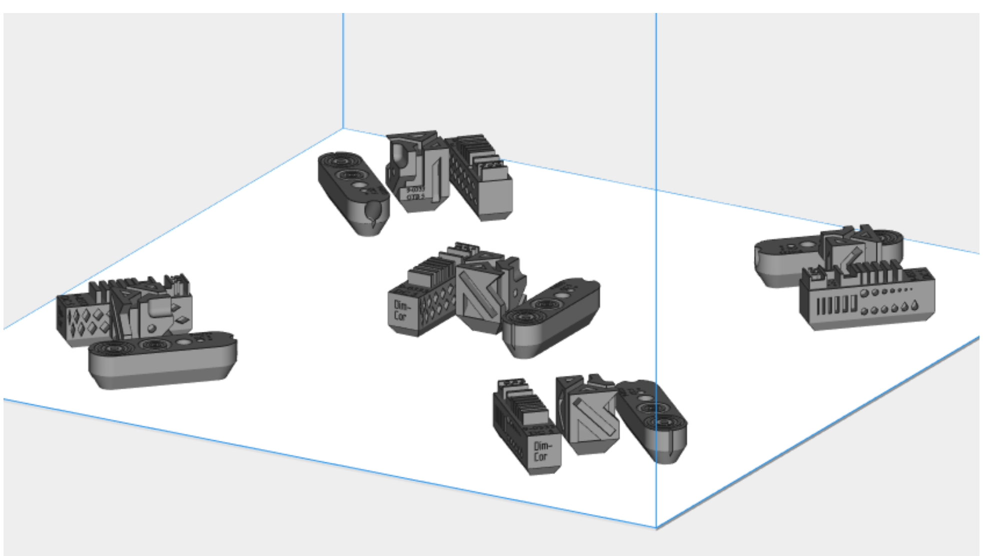

SIDE 1

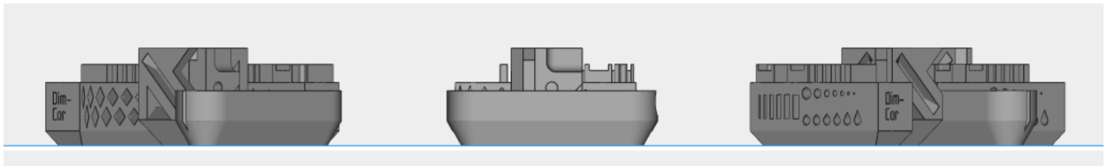

SIDE 2

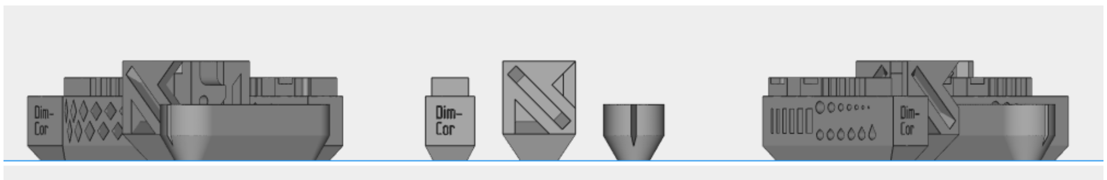

SIDE 3

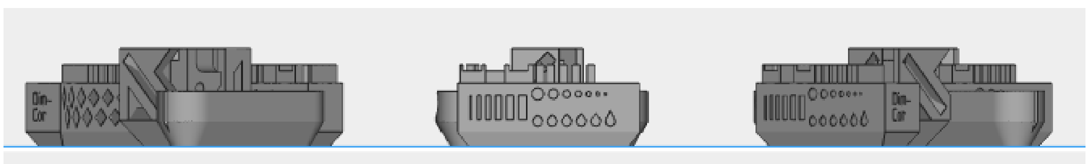

SIDE 4

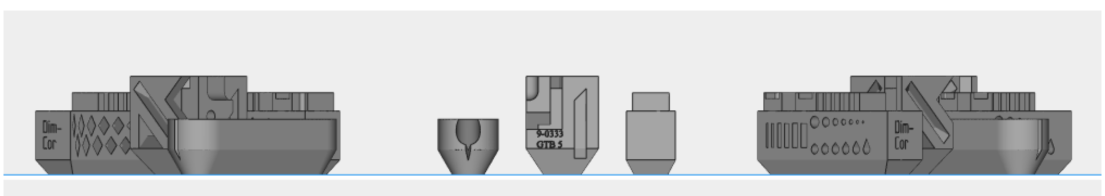

Segment 1-5

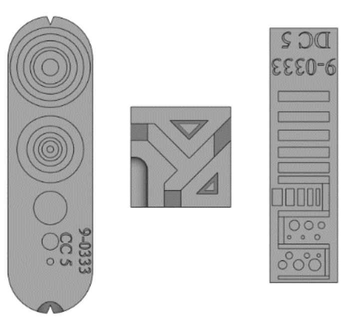

Structured Light Dimensional Analysis

Each dimensional test block underwent structured light dimensional analysis to determine the effects of part location on build plate and recoater/gas flow direction on geometric accuracy. Statistics for maximum deviation from nominal geometry (based on the test block from the center of the build bed) are included for each test block below. Full details of the structured light scans can be found in the attached reports.

Contour Check

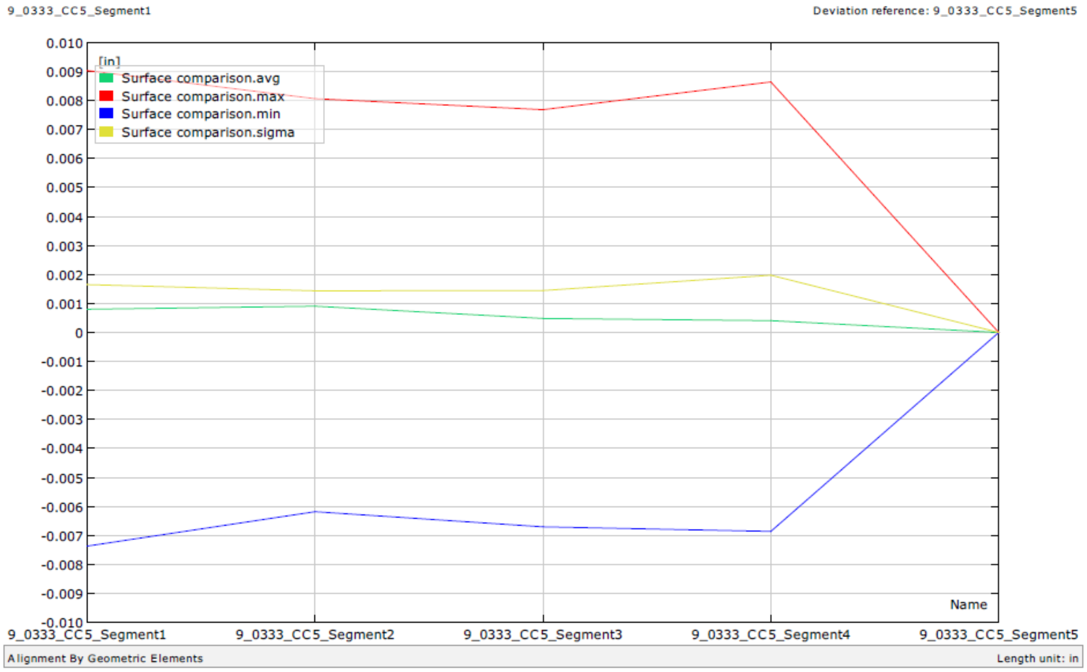

Dimensional Corner

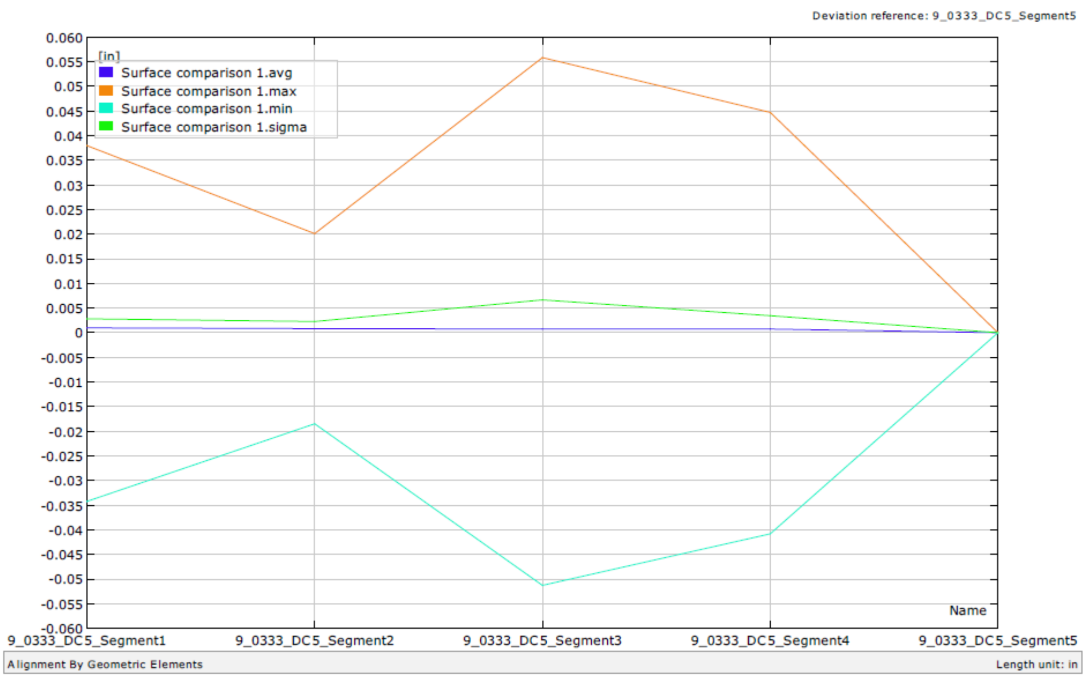

Geometry Test Block

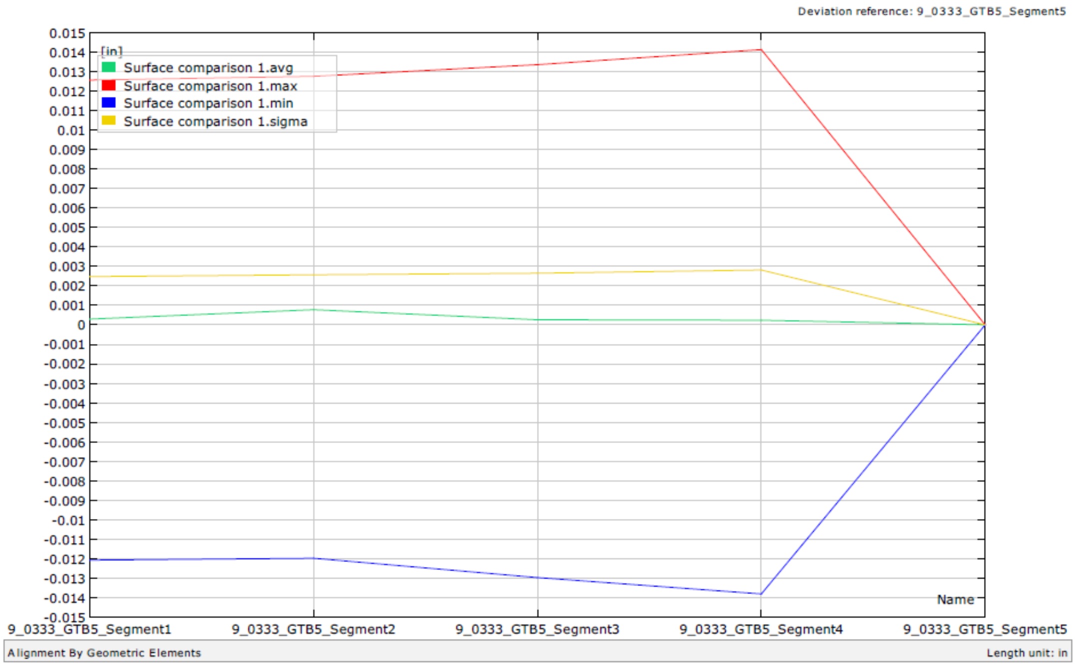

Build Set Utilized: 2021-0230 QMP Build 1

Overall Layout

TOP

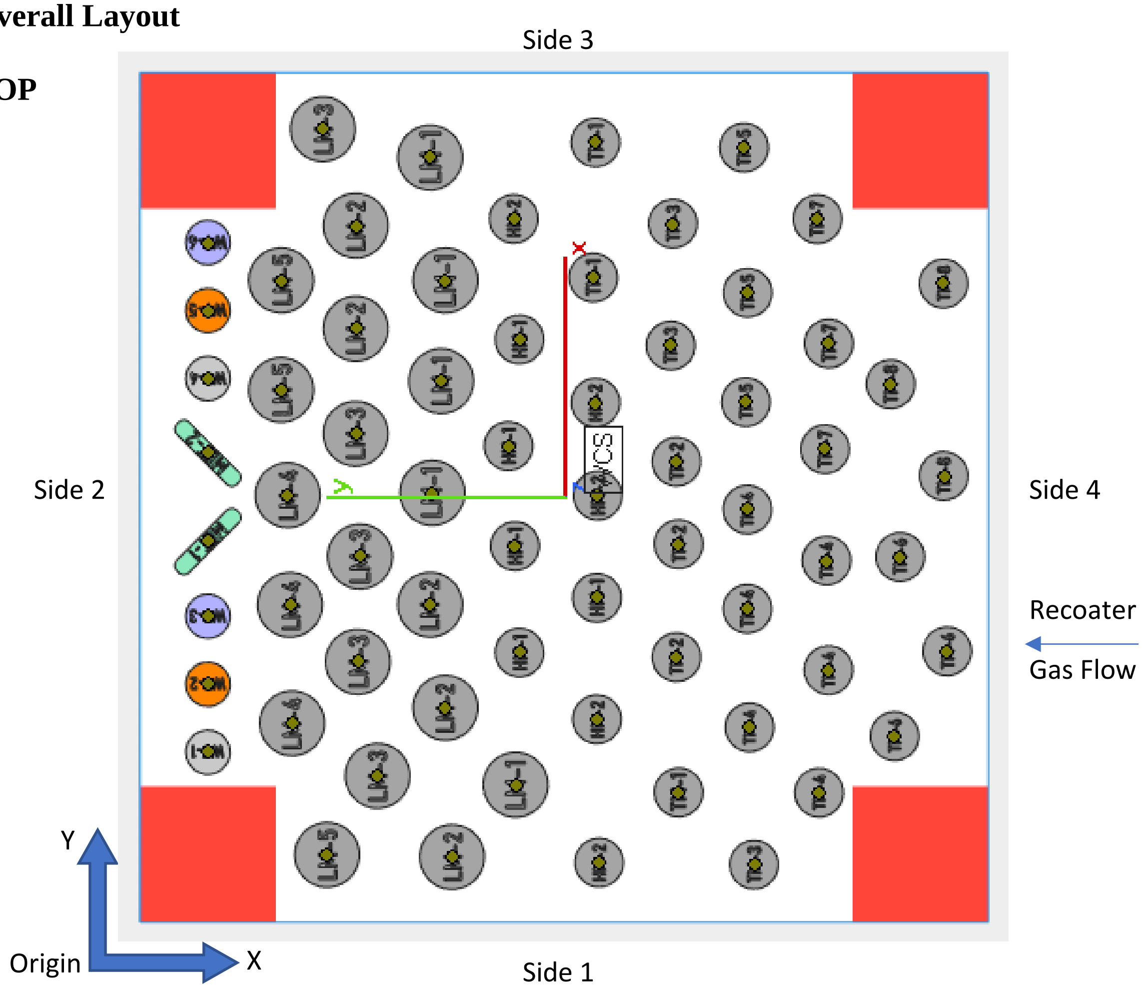

It was discovered during mechanical testing of the specimens in Build 1 that specimen names were inadvertently duplicated during the build process due to operator error. This limits traceability of the specimens back to a specific location on the build plate. Additional numbered suffixes were added to the specimen names at the mechanical testing stage to differentiate the specimens.

QMP Builds 2, 3, and 4 failed due to defects caused by the use of a rubber recoater blade. Build 5 resumed use of steel recoater blade.

Recoater Test Build 1 – Steel Blade

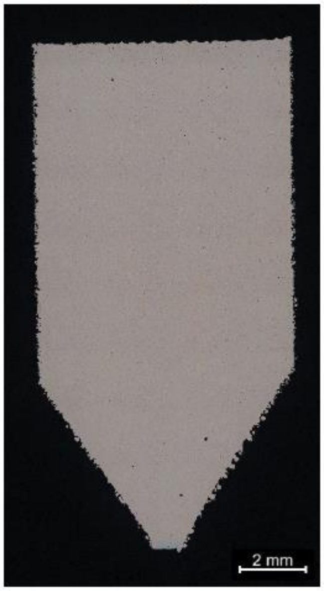

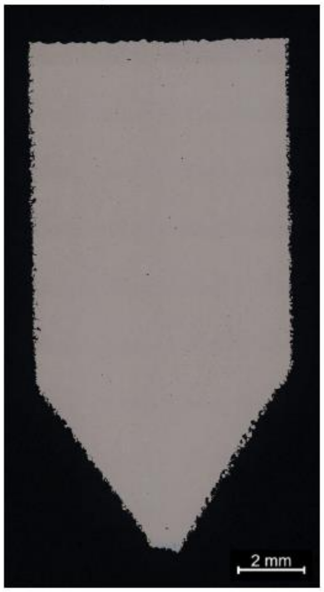

Three specimens produced using a steel recoater blade were examined for gross defects. No streaks from the recoater blade were observed. Minimal large defects and minor banding previously tied to the ventilator were observed.

Recoater Test Build 2 – Rubber Blade

Three specimens using a rubber recoater blade were examined for defects. The same build parameters were used for both test build 1 and test build 2. Recoater tracks were observed in the top surface and large lack of fusion defects due to recoater blade issues were observed.

Build Set Utilized: 2021-0276 Thin Section Study

Overall Layout

TOP

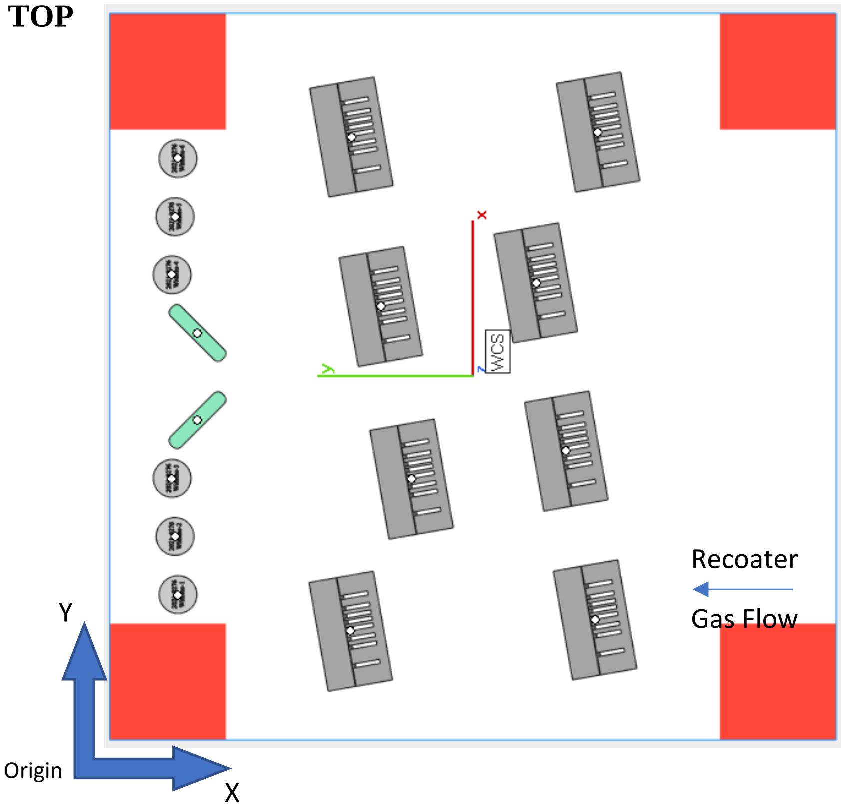

ISO

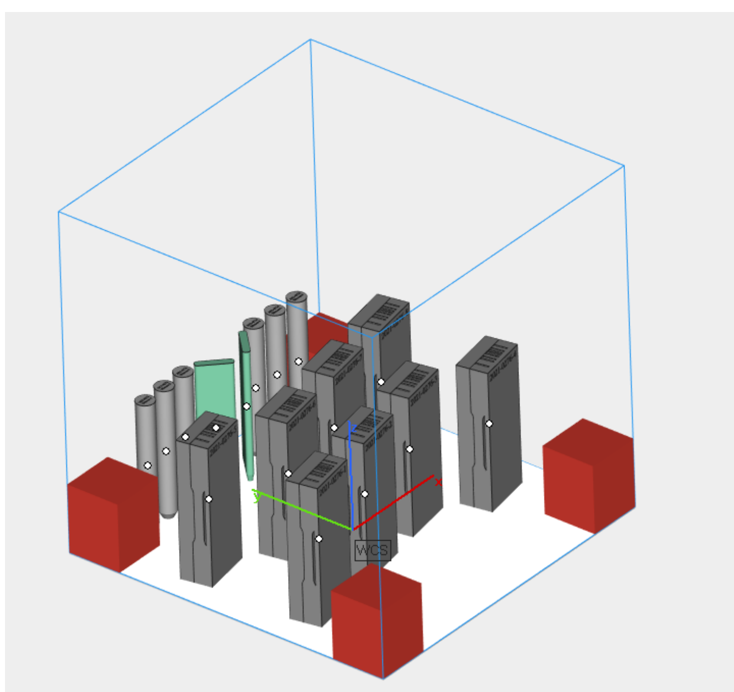

Build Set Utilized: 2021-0392 QMP Build 5

Overall Layout

TOP

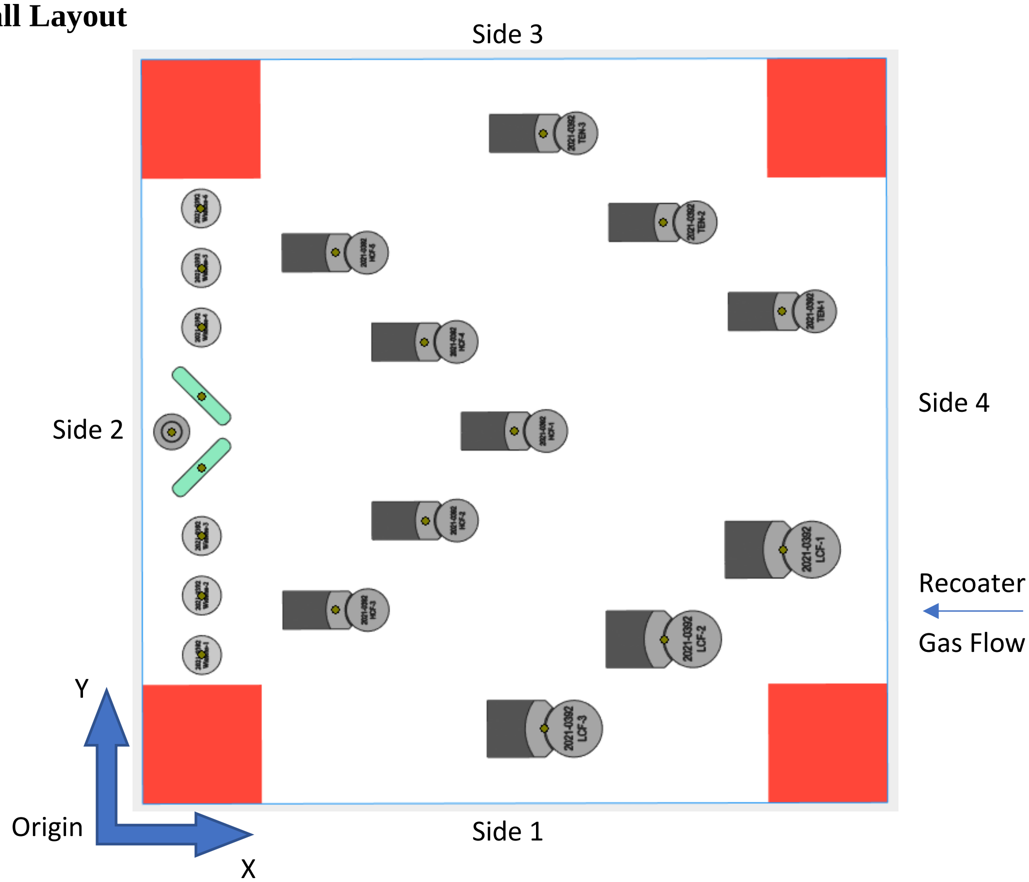

ISO

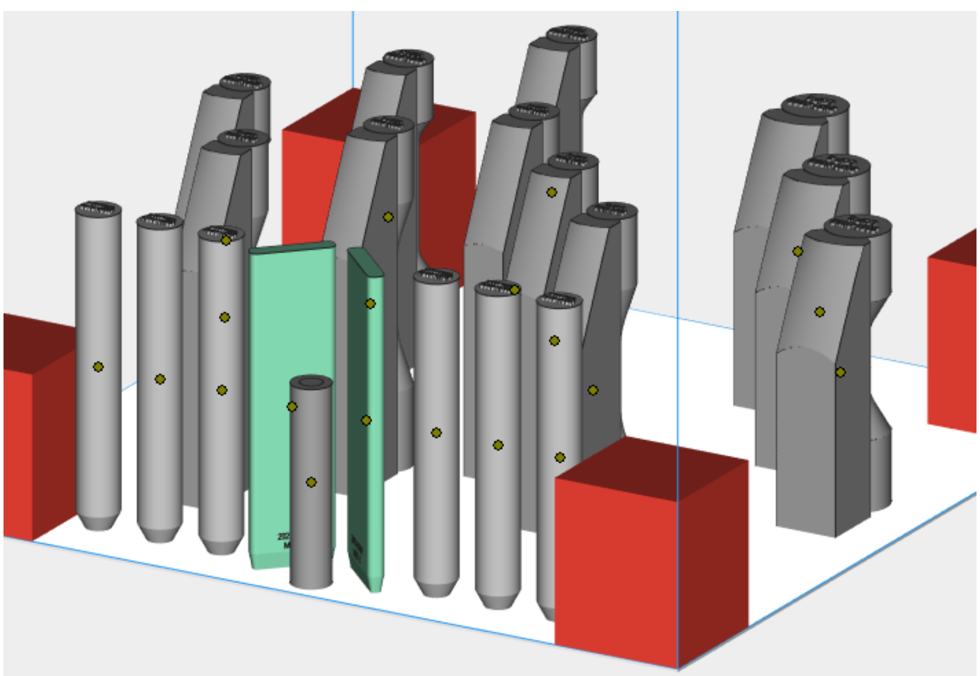

SIDE 1

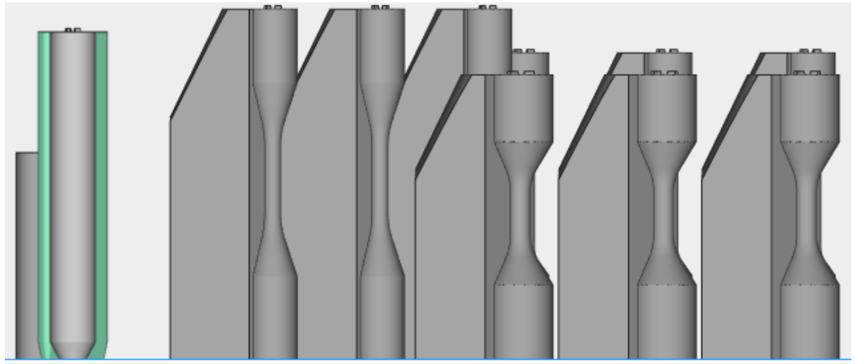

SIDE 2

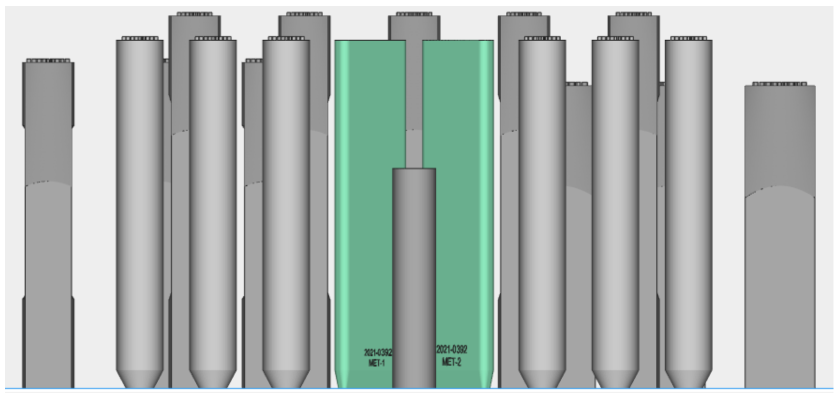

SIDE 3

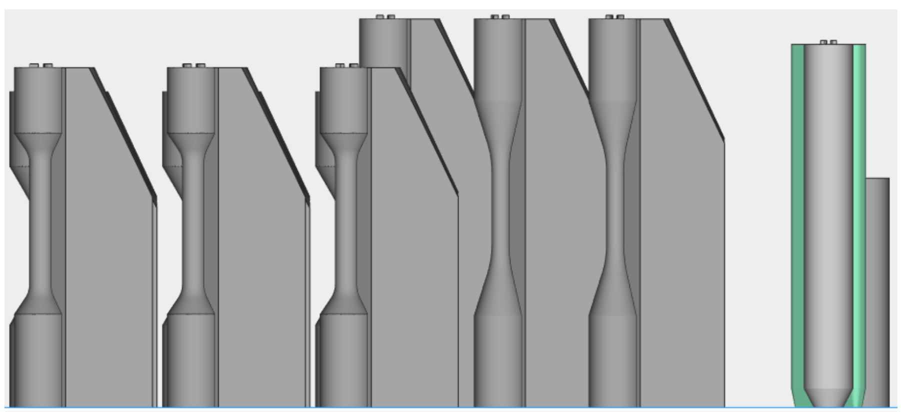

SIDE 4

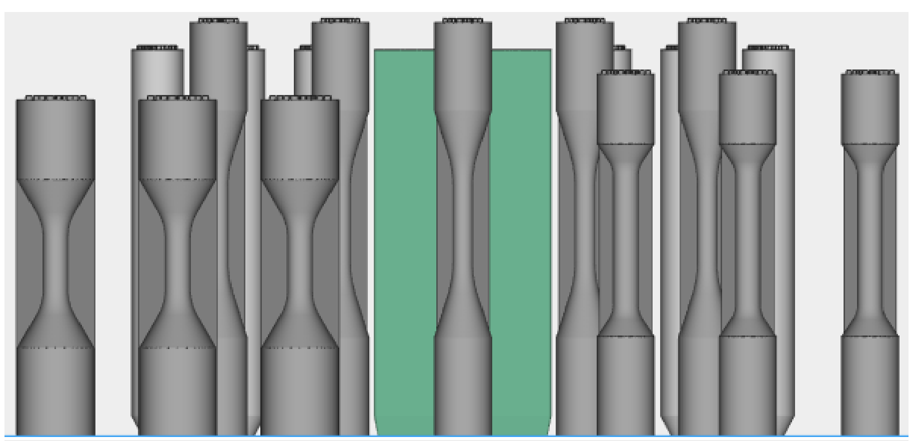

Build Set Utilized: 2021-0393 QMP Build 6

Overall Layout

TOP

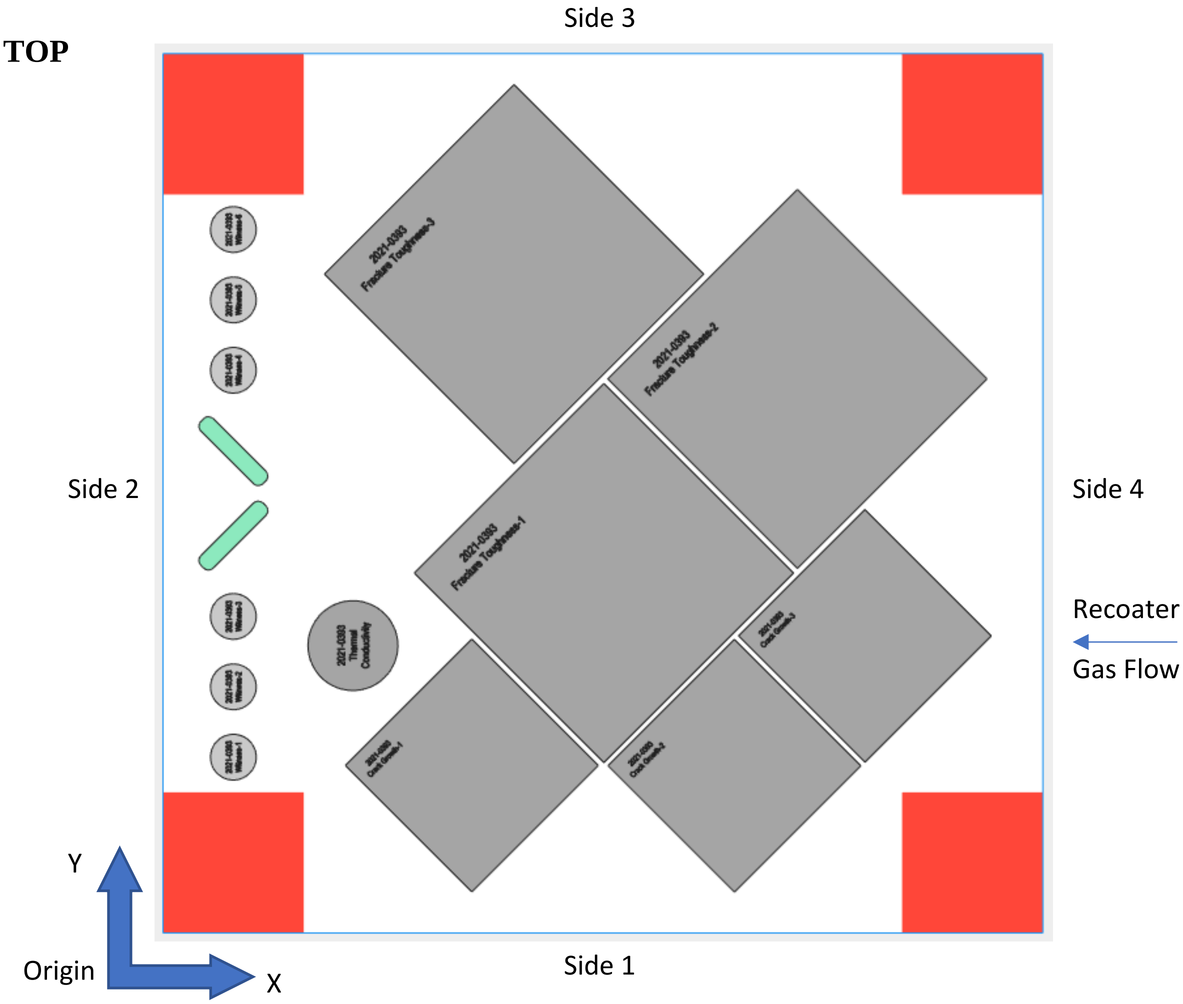

ISO

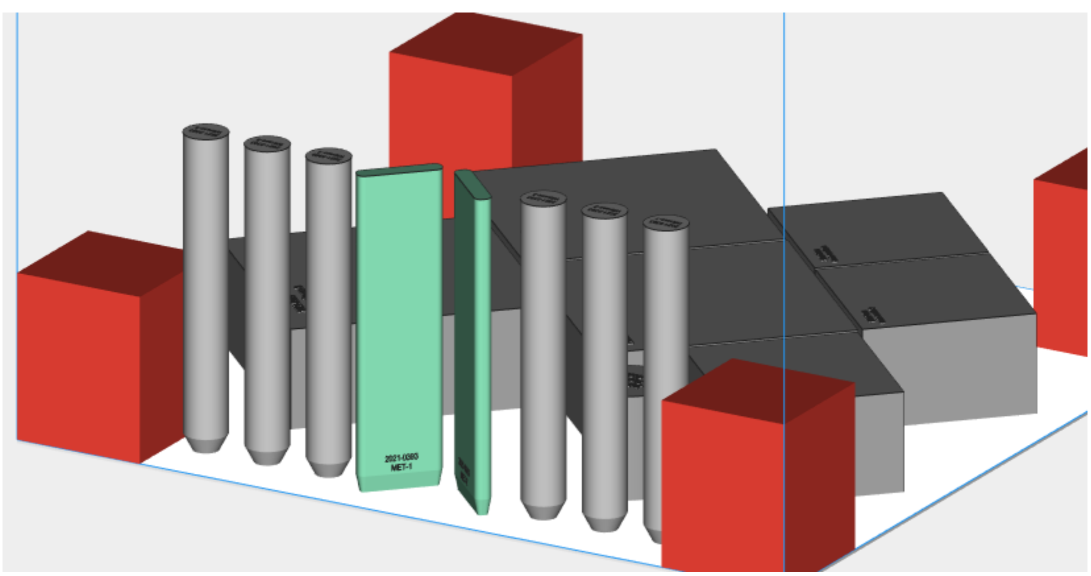

SIDE 1

SIDE 2

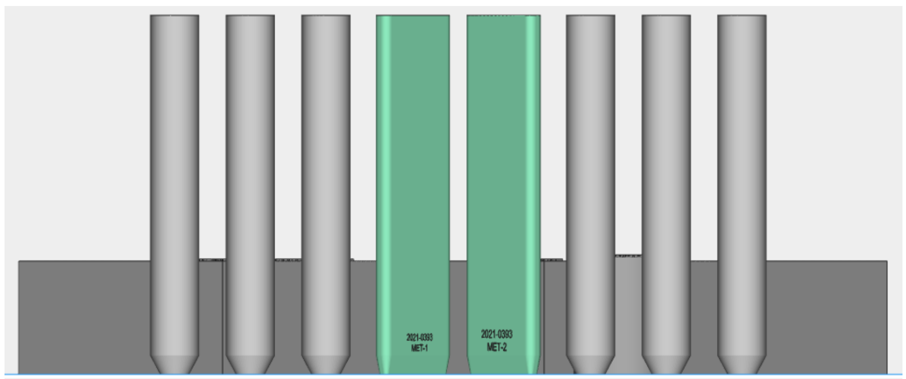

SIDE 3

SIDE 4

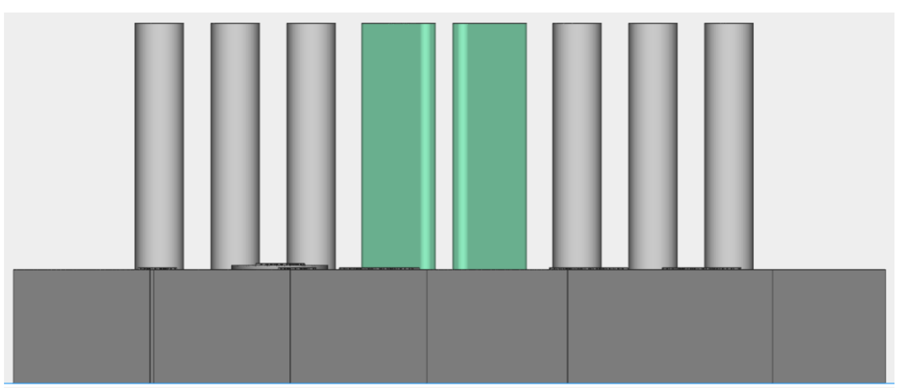

Build Set Utilized: 2021-0406 QMP Build 7
Overall Layout

TOP

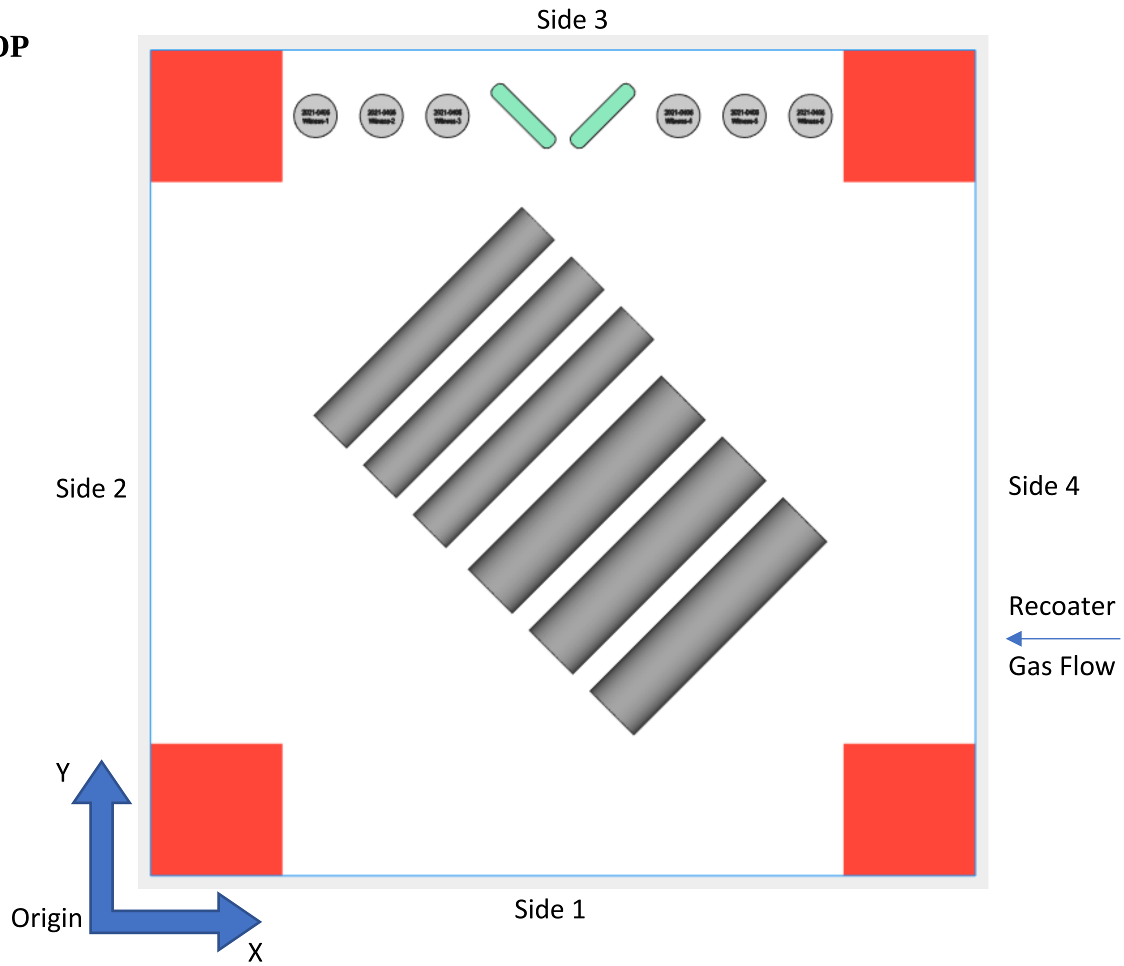

ISO

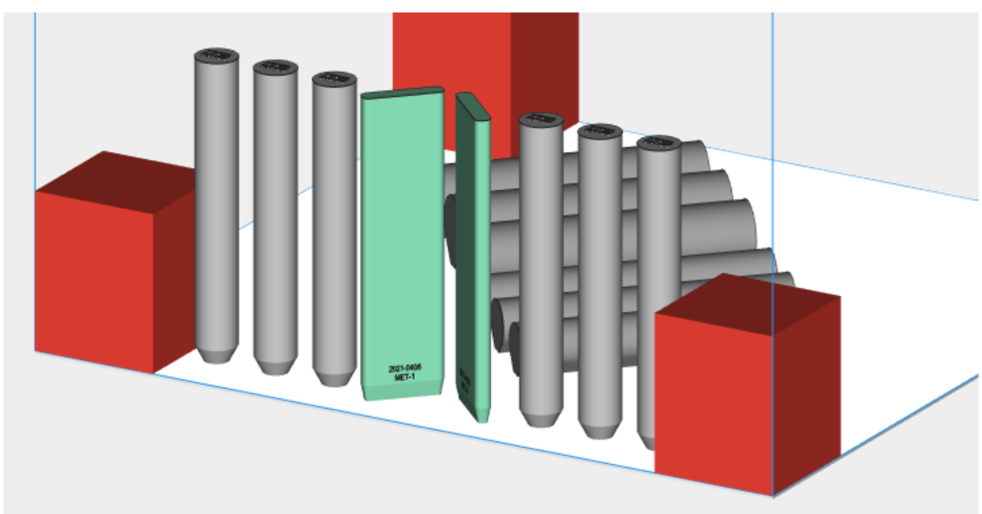

SIDE 1

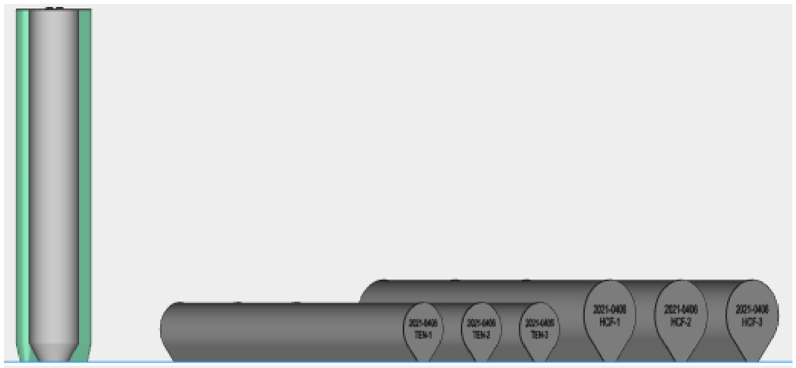

SIDE 2

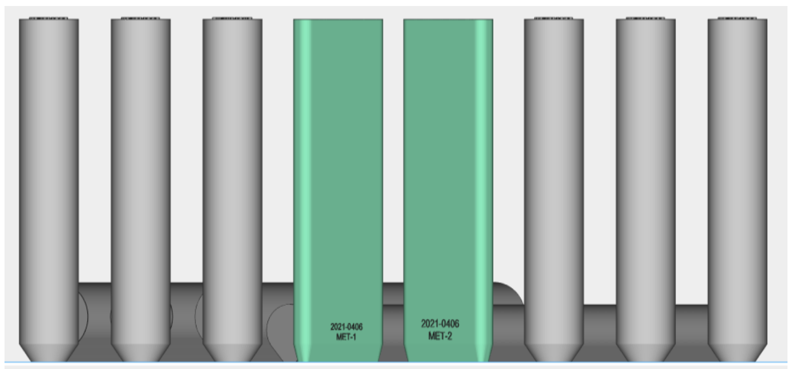

SIDE 3

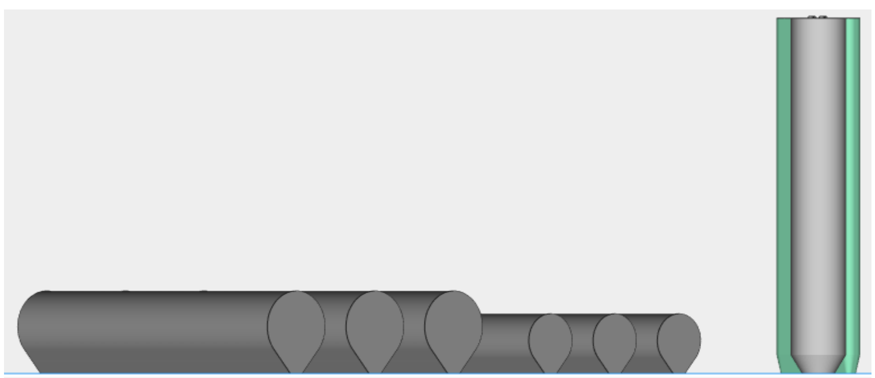

SIDE 4

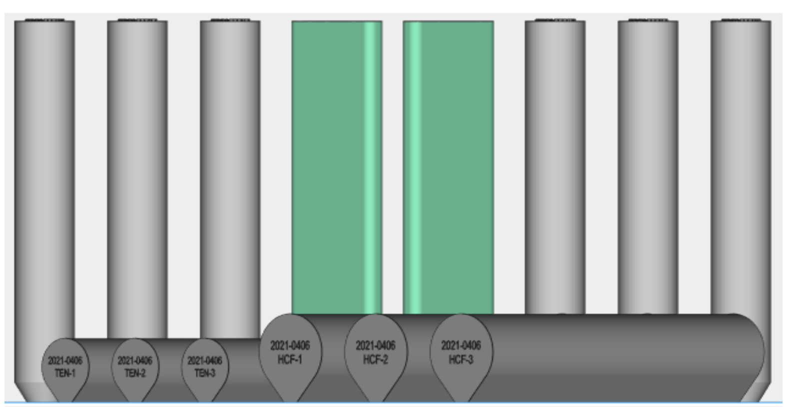

As Built and Heat-Treated Microstructure Evaluations

<table>
<tr><th colspan="2">Build Area Survey</th></tr>
<tr><th colspan="2">2021-0230 QMP Build 1</th></tr>
<tr><td colspan="2">As-built Microstructure Evaluation:</td></tr>
<tr><td colspan="2">No as-built specimens were received for Build 1. All microstructural evaluation specimens received for this build were in the post-HIP condition.</td></tr>
<tr><td colspan="2">Heat-treated Microstructure Evaluation:</td></tr>
<tr><td>Magnification</td><td>100x</td></tr>
<tr><td colspan="2">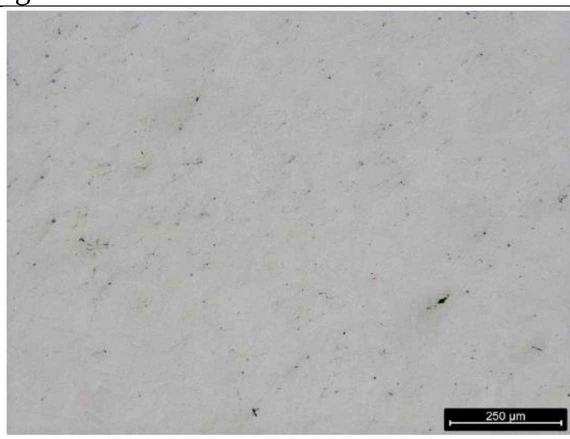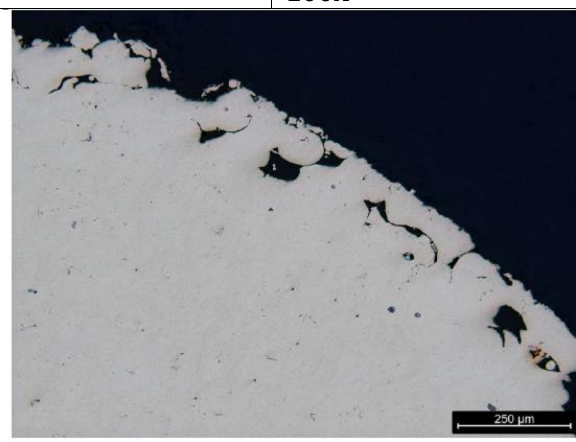
Lack of Fusion Defects in Core Contour Defects at Edges
Lack of fusion defects in the core were on the high end for post-HIP material.</td></tr>
<tr><th colspan="2">2021-0392 QMP Build 5</th></tr>
<tr><td colspan="2">As-built Microstructure Evaluation:</td></tr>
<tr><td>Plane</td><td>Z and XY Planes</td></tr>
<tr><td>Magnification</td><td>100x</td></tr>
<tr><td colspan="2">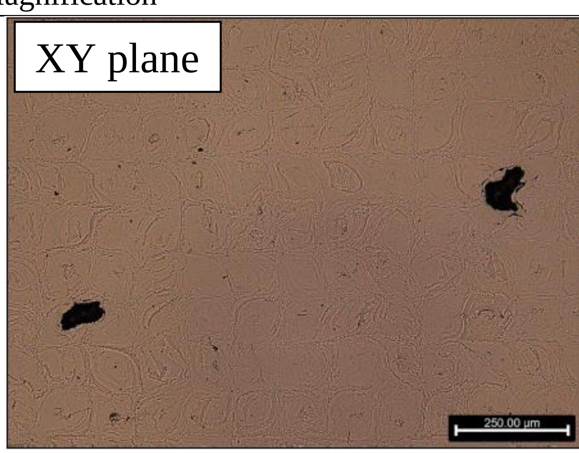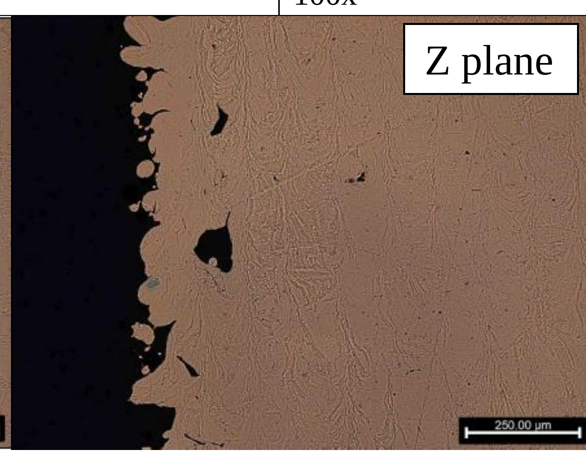
Lack of Fusion Defects in Core Contour Defects at Edges

Acceptance Statement:
Images shown demonstrate that defects of note are minimal and are consistent with the expected maximum size for isolated defects in a nominal process.</td></tr>
</table>

Heat-treated Microstructure Evaluation:	
Plane	Z Plane
Magnification	100x

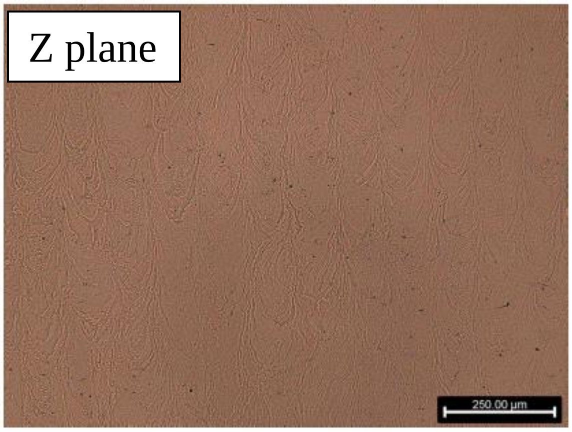

No core defects noted

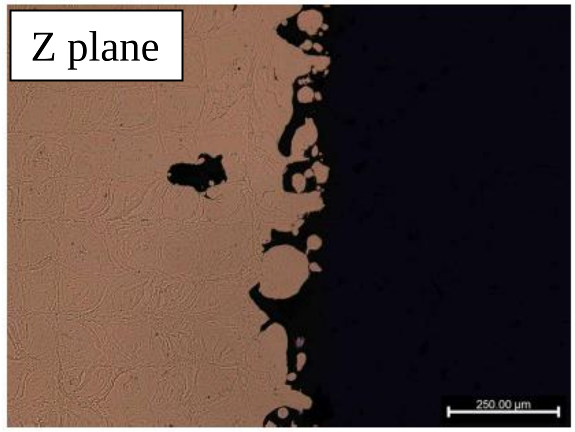

Contour Defects at Edges

Acceptance Statement:
Images shown demonstrate that defects of note are minimal and are consistent with the expected maximum size for isolated defects in a nominal process.

2021-0393 QMP Build 6

As-built Microstructural Evaluation:

Plane	Z Plane
Magnification	100x

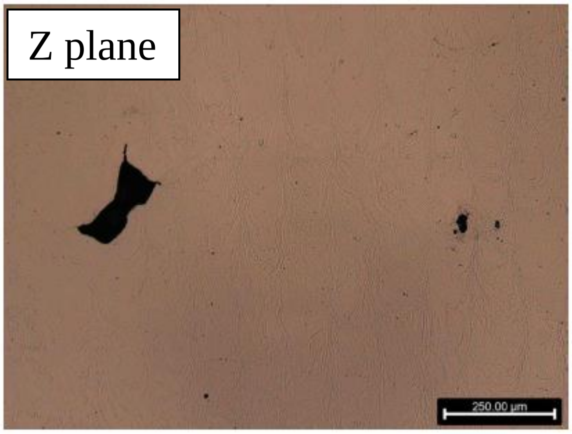

Lack of Fusion Defects in Core

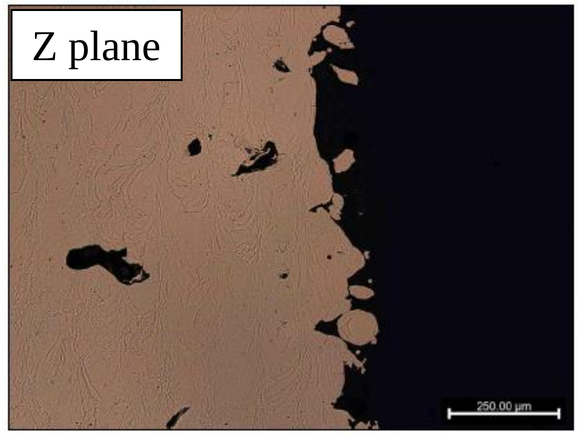

Contour Defects at Edges

Acceptance Statement:
Images shown demonstrate that defects of note are minimal and are consistent with the expected maximum size for isolated defects in a nominal process.

Heat-treated Microstructural Evaluation:

Plane	Z Plane
Magnification	100x

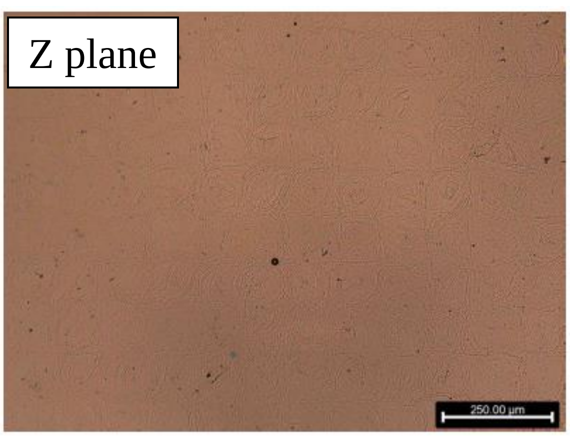

Possible Lack of Fusion Defects in Core

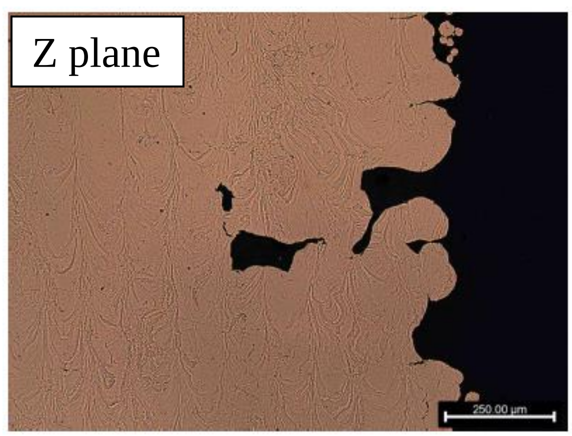

Contour Defects at Edges

Acceptance Statement:
Images shown demonstrate that defects of note are minimal and are consistent with the expected maximum size for isolated defects in a nominal process.

2021-0406 QMP Build 7

As-built Microstructural Evaluation:

Plane	Z and XY Planes
Magnification	100x

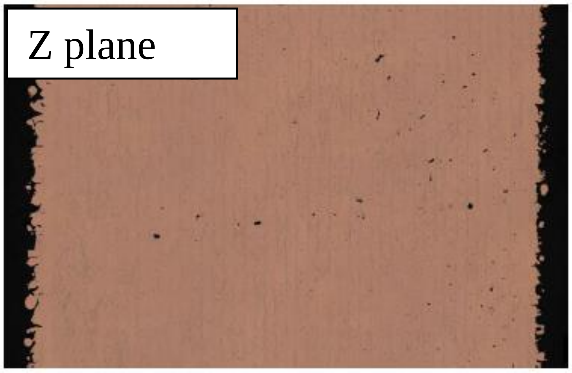

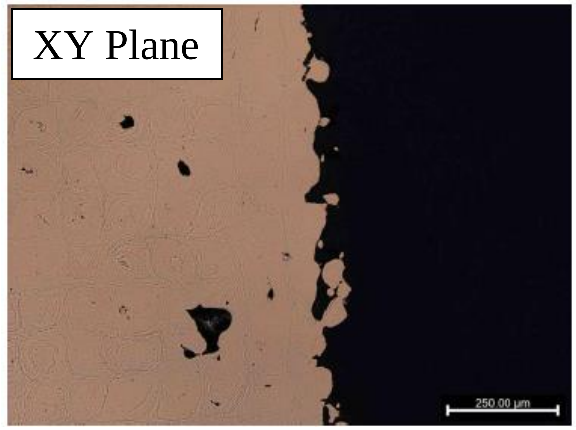

Banding Defects in the As-built Material

Contour Defects at Edges

Acceptance Statement:
Banding defects were present in as-built material, typical for as-built parts produced with the M2. These defects are small and isolated enough to be of no concern after heat treatment.

Heat-treated Microstructural Evaluation:

Plane	Z Plane
Magnification	100x

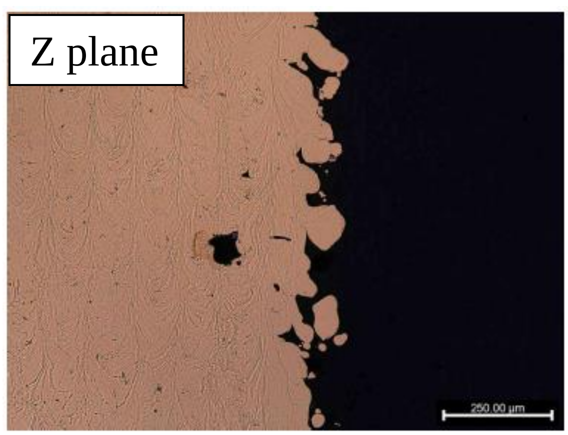

Isolated Contour Defects at Specimen Edges

Acceptance Statement:
Images shown demonstrate that defects of note are minimal and are consistent with the expected maximum size for isolated defects in a nominal process.

Across all builds, defects were generally small and isolated and consistent with those expected for parts manufactured on the M2. HIP was generally effective at closing significant core defects existing in the as-built condition.

2021-0276 Thin Section Study

As-built Microstructural Evaluation:	
Plane	XY Plane
Magnification	100x

The thin wall specimens were observed to have significant contour defects through the samples with intermittent banding defects found in the core of each. Some isolated larger defects were observed in some samples, including the thinnest bar, that may influence tensile properties if unresolved during HIP.

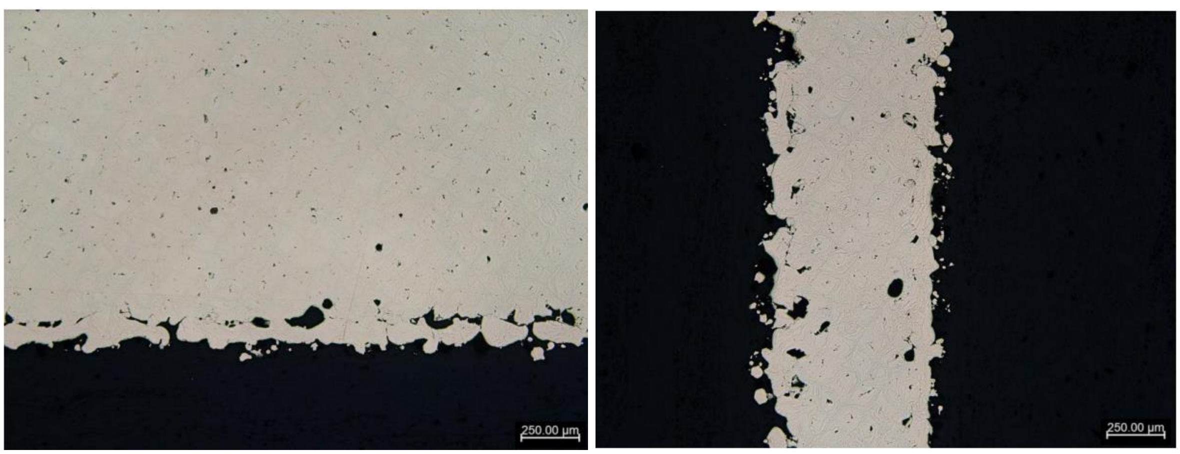

As-built Microstructural Evaluation:	
Plane	XZ Plane
Magnification	100x

In the XZ plane of the gauge sections, all the thin section samples had poor contour adhesion on at least one side. This may influence the tensile results as the actual load bearing area will be smaller than measured with calipers or point mics. Banding defects were observed with varying severity in the different sample thicknessess wich may heavily influence the test results, particularly for the thinnest samples if not resolved during HIP.

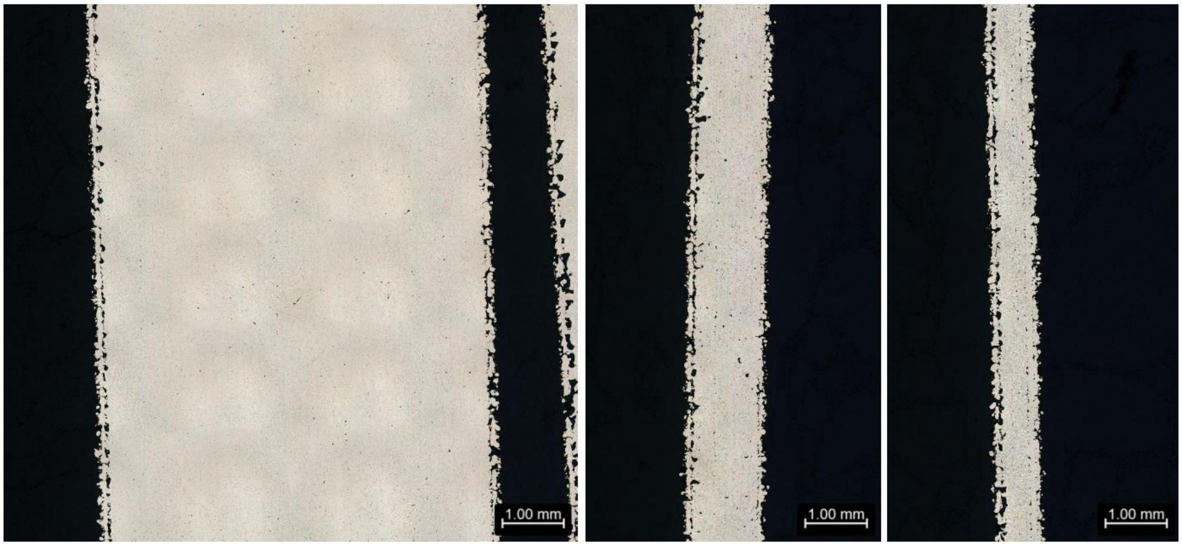

Suspect: Significant contour defects throughout the as-built samples may not be resolved by HIP. Presence of numerous linear defects may impact the tensile tests by increasing scatter on the test results or resulting in significantly fracture elongation and/or strengths.

Heat-treated Microstructural Evaluation:	
Plane	XY and XZ Planes
Magnification	100x, 200x, 500x

Metallography was not performed on heat-treated thin sections, but instead on a HIP'd metallography witness bar produced in the same build as the thin-wall blocks. Large contour defects were noted in the heat-treated metallography bars.

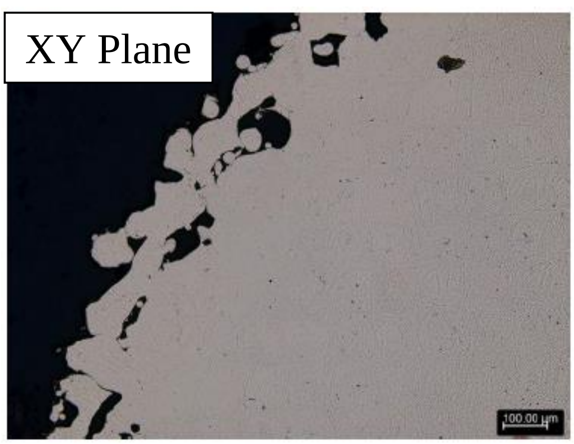

Contour Defects on Rounded Edge

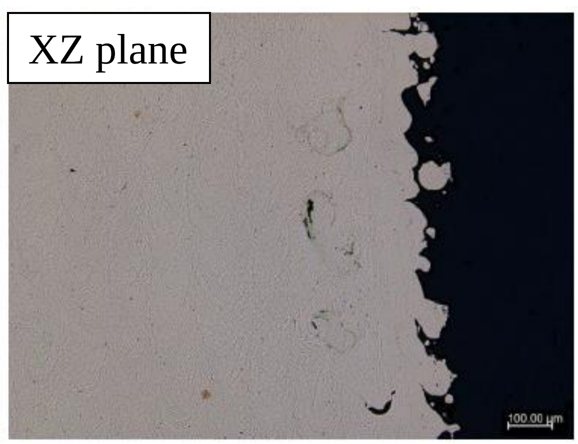

Contour Defects Below Polished Surface

Coarse Cr_2Nb precipitates were observed in the HIP metallography bar, making it impossible to obtain accurate porosity measurements. Porosity in the HIP condition is estimated to be lower than in the as-built condition.

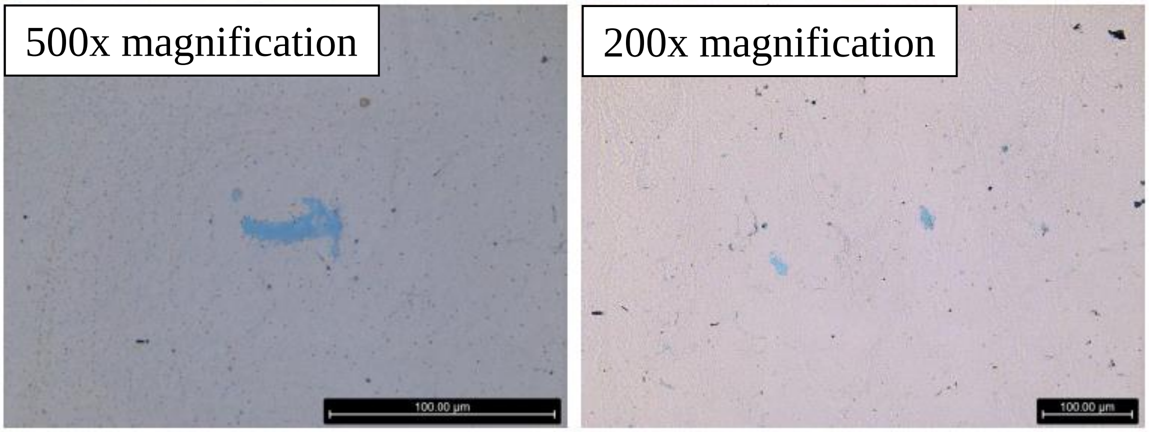

Coarse Cr_2Nb precipitates in the HIP metallography witness bar

Mechanical Properties

1. Tensile

Tensile tests were conducted in lab air at room temperature following procedures in ASTM E8. 33 specimens were machined after HIP using standard shop procedures, while three HIP specimens were left in the as-built surface condition to investigate the effect of surface roughness on tensile properties. Specimens were produced either with the longitudinal axis running parallel to the build direction ("Z") or perpendicular to the build direction ("XY"). Summaries of the tensile results are listed in Table 1. Figure 1 shows typical tensile curves. Individual results for each specimen are listed in Appendix 2.

Table 1. Room temperature tensile results summary – machined finish

		Ult. Ten. Strength (ksi)		**Yield Strength (ksi)**		**Fracture Elong. (%)**	
Group	**Count**	**Av.**	**Std. Dev.**	**Av.**	**Std. Dev.**	**Av.**	**Std. Dev.**
All	33	53.9	1.02	28.6	0.92	29.6	1.59
Z Only	30	53.7	0.69	28.4	0.57	29.6	1.67
XY Only	3	56.4	0.09	30.9	0.08	29.4	0.08

Table 2. Room temperature tensile results summary – as-built finish

		Ult. Ten. Strength (ksi)		**Yield Strength (ksi)**		**Fracture Elong. (%)**	
Group	**Count**	**Av.**	**Std. Dev.**	**Av.**	**Std. Dev.**	**Av.**	**Std. Dev.**
All	3	49.1	0.12	25.1	0.12	30.7	2.75

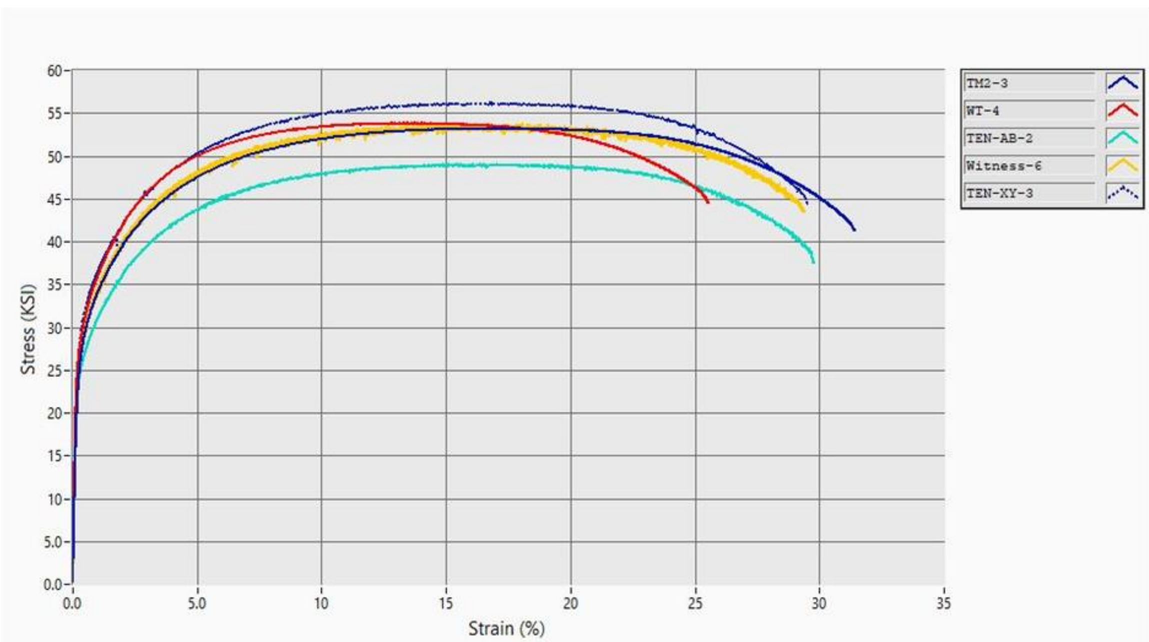

Figure 1. Typical room temperature tensile curves.

Table 1 shows results from the combined tensile data set of machined specimens ("All") and then shows subsets of the results separated by orientation. The XY-oriented specimens exhibited higher strength than the Z-oriented specimens, and also exhibited lower standard deviation. The highest standard deviation in tensile and yield strengths is observed in the "All" group, likely reflecting the observed strength differences between Z- and XY-oriented specimens. Note that the averages reported in Table 1 do not account for an outlying specimen (Specimen WT-1, which is discussed in detail in Appendix 2). Table 2 shows results from the dataset of tensile specimens with the as-built surface finish. All as-built tensile specimens were Z-oriented. The as-built specimens exhibit reduced average tensile and yield strengths but increased average elongation compared to machined-finish specimens.

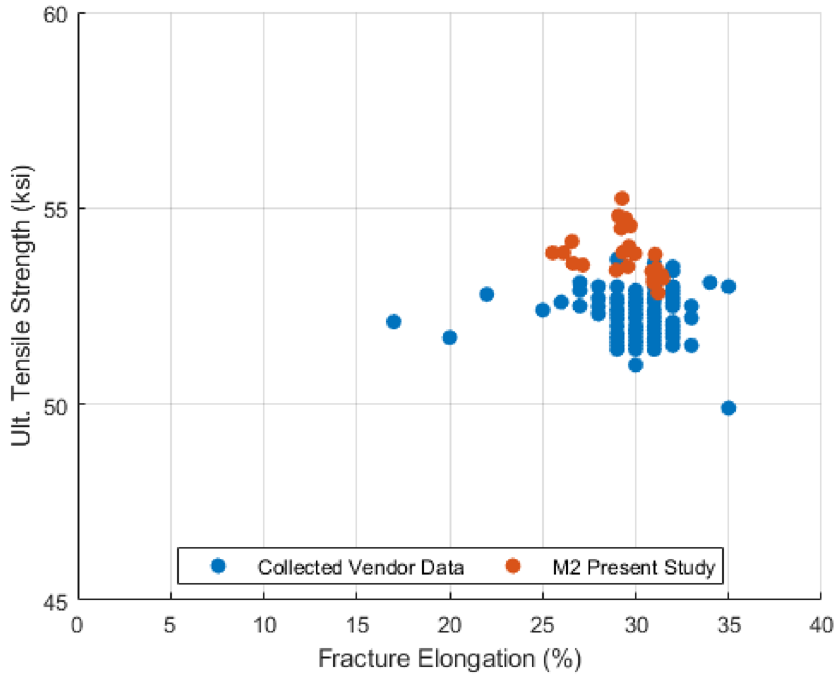

Figure 2. Present study ultimate tensile strength vs fracture elongation compared to data collected by MSFC for multiple vendors and machines – Z-oriented specimens at 70˚ F.

Figure 2 shows the ultimate tensile strength and fracture elongation values from the Z-oriented, machined specimens tested at 70˚ F in the present study compared against comparable data collected by MSFC for multiple vendors and machines. Results from the present study have a higher average tensile strength and reduced standard deviation in the fracture elongation compared to existing data. It is suspected that this discrepancy is due to differences in powder specifications, build machine, and processing parameters between the present study and previously compiled work.

Figure 3 compares the Z-oriented specimens from the present study to reference distributions developed from tensile data previously collected by MSFC. Specimens in the present study exhibit higher strength values relative to the previously collected data. The present study specimens exhibit fracture elongation values comparable to the previously collected data.

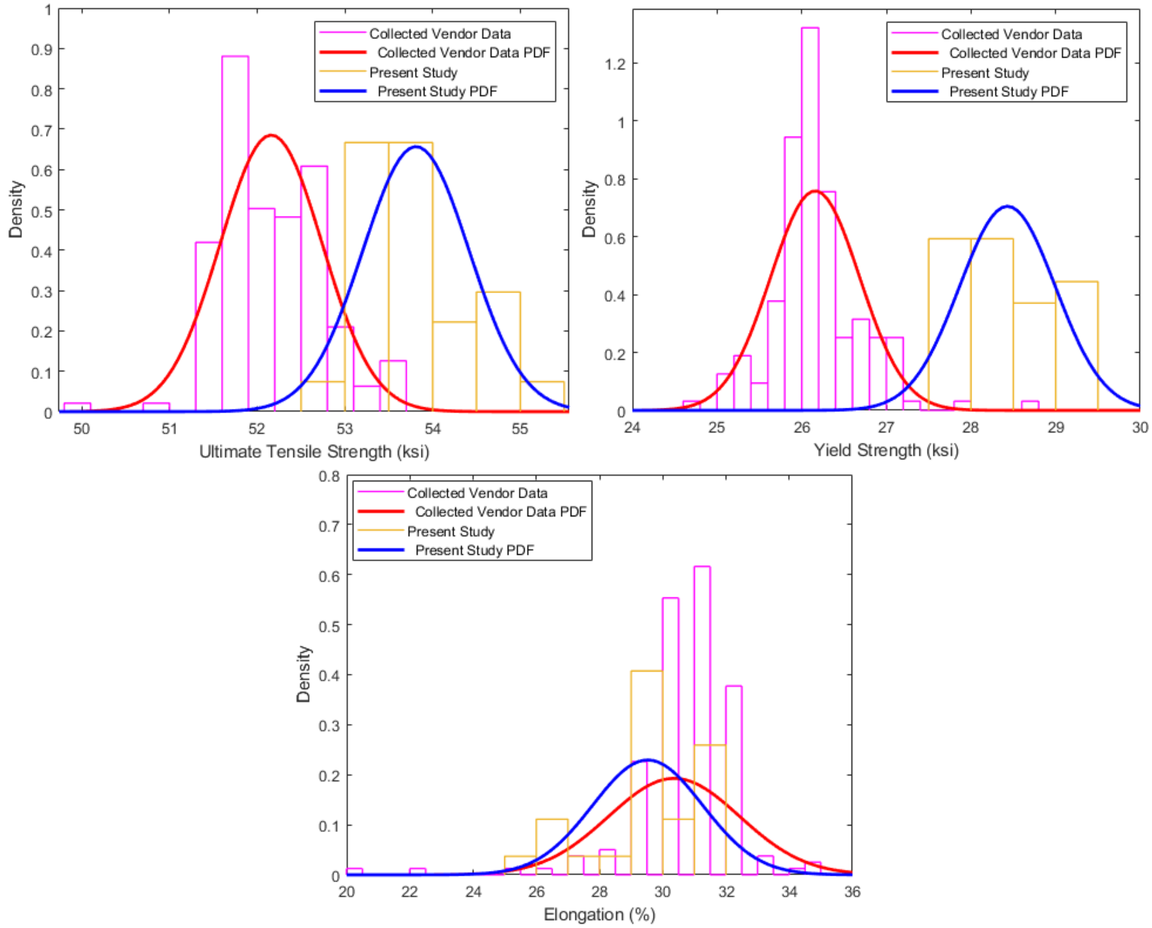

Figure 3. Reference distribution plots for the M2 Z-oriented specimens in the present study compared to data collected by MSFC from multiple machines and vendors.

Tensile tests were also conducted on machined-finish Z-orientation specimens at elevated temperatures following procedures in ASTM E21. All specimens were machined following standard shop procedures. All elevated temperature specimens were produced with the longitudinal axis running parallel to the build direction ("Z"). Summaries of the elevated temperature tensile results are listed in Table 3. Elevated temperature tests were performed in lab air; specimens were soaked at the elevated temperature for 15 minutes before commencement of the test. Figure 4 shows typical tensile curves. Individual results for each specimen are listed in Appendix 2.

Table 3. Elevated temperature tensile results summary

		Ult. Ten. Strength (ksi)		**Yield Strength (ksi)**		**Fracture Elong. (%)**	
Group	**Count**	**Av.**	**Std. Dev.**	**Av.**	**Std. Dev.**	**Av.**	**Std. Dev.**
750˚ F	3	28.1	0.15	21.7	0.09	21.5	0.57
1112˚ F	3	18.0	0.23	16.7	0.12	39.8	2.32

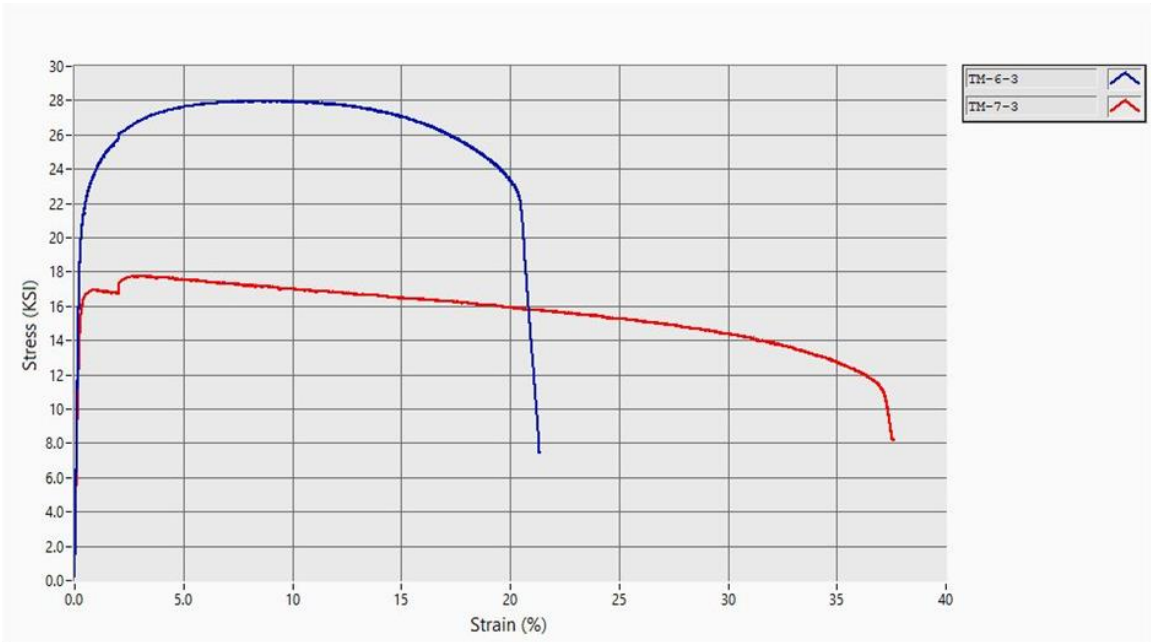

Figure 4. Typical elevated temperature stress-strain curves. Specimen TM-6-3 was tested at 750˚ F; Specimen TM-7-3 was tested at 1112˚ F.

Table 3 shows results from the elevated temperature data set. As expected, tensile and yield strengths decreased with increased temperature, exhibiting a 47% reduction in average tensile strength compared to room temperature at 750˚ F and a 66% reduction in average tensile strength compared to room temperature at 1112˚ F. Average elongation to failure decreased by 24% compared to room temperature at 750˚ F, but increased by 40% compared to room temperature at 1112˚ F. This intermediate temperature ductility trough has been previously observed in GRCop-84 and other copper alloys[1,2].

2. Tensile Thin Walls

Sixty-three (63) thin section specimens were tested based on the guidelines established in ASTM E8, Standard Test Methods for Tension Testing of Metallic Materials, and per customer direction. The specimens had a nominal gage section width of 0.25 inch and a nominal reduced section length of 1.25 inches.

[1] Ellis, David L., Loewenthal, William S., and Yun, Hee Man, Tensile Properties of GRCop-84. NASA Technical Report TM-2012-217108, NASA Glenn Research Center, Cleveland, OH, 2012.

[2] Laporte, V. and Mortensen, A., Intermediate Temperature Embrittlement of Copper Alloys. International Material Reviews Vol. 54 No. 2, 2009.

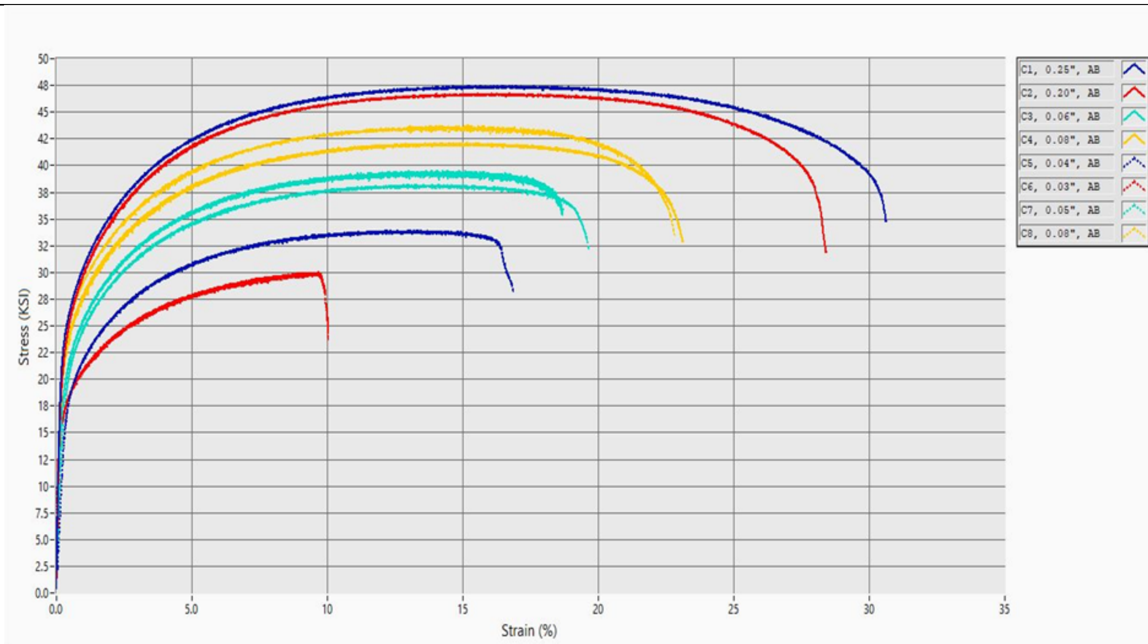

Figure 5. Representative stress-strain plots for thin-wall tensile specimens

Table 4. Room temperature tensile results summary – thin walls

		Ult. Ten. Strength (ksi)		**Yield Strength (ksi)**		**Fracture Elong. (%)**	
Thickness	**Count**	**Av.**	**Std. Dev.**	**Av.**	**Std. Dev.**	**Av.**	**Std. Dev.**
0.03”	7	29.39	1.76	16.23	0.41	11.42	4.40
0.04”	7	33.64	1.19	18.66	0.41	14.89	4.41
0.05”	7	37.58	0.38	20.31	0.44	18.28	2.87
0.06”	7	39.40	0.36	20.84	0.65	19.19	2.02
0.08”	7	41.71	0.29	22.06	0.50	21.34	2.64
0.10”	7	43.35	0.31	22.51	0.94	22.47	2.79
0.20”	7	46.74	0.34	24.17	0.76	26.66	2.69
0.25”	14	47.53	0.22	24.78	0.30	28.65	1.75

It is observed that tensile strength, yield strength, and fracture elongation decrease with each decrease in wall-thickness, consistent with trends observed in previous studies of GRCop-42 and other AM alloys[34]. Per NASA-STD-6030, the effects of wall thickness on mechanical property debits are to be accounted for through the use of influence factors when developing design values. Figure 5 presents stress-strain curves for the thin wall specimens, while Table 4 summarizes the mechanical properties. Mechanical property data for individual thin-wall tensile specimens can be found in Appendix 3.

3. High Cycle Fatigue

Five round fatigue specimens were tested according to ASTM E466 *Standard Practice for Conducting Force Controlled Constant Amplitude Axial Fatigue Tests of Metallic Materials.* All specimens were tested in the as-built surface finish and oriented in the Z direction. Testing conditions were 70° F ambient lab air and a stress ratio of R=0.1. Cyclic loading was applied at 40 Hz in a tapered sine waveform. Specimens had a nominal reduced section length of 0.75 in and 0.2 in nominal gage diameter. Tests were run until specimen failure or 10,000,000 cycles, whichever occurred first. Table 5 lists the results of the HCF testing, and Figure 6 shows the stress-life curve for the specimens.

Table 5. HCF Results

Specimen	Max Stress (ksi)	Alt. Stress (ksi)	Cycles to Failure
HCF-AB-1	18	8.1	10,000,000
HCF-AB-2	23	10.35	3,827,726*
HCF-AB-3	25	11.25	796,935
HCF-AB-4	27	12.15	787,667
HCF-AB-5	23	10.35	2,248,986

*HCF-AB-2 continued to cycle after failure due to the failure detector's sensitivity not being set low enough. Cycling was stopped at cycle count 3,827,726. The last recorded data cycle occurred at cycle 2,000,000. The true cycle count of HCF-AB-2 is between 2,000,000 and 3,827,726 cycles.

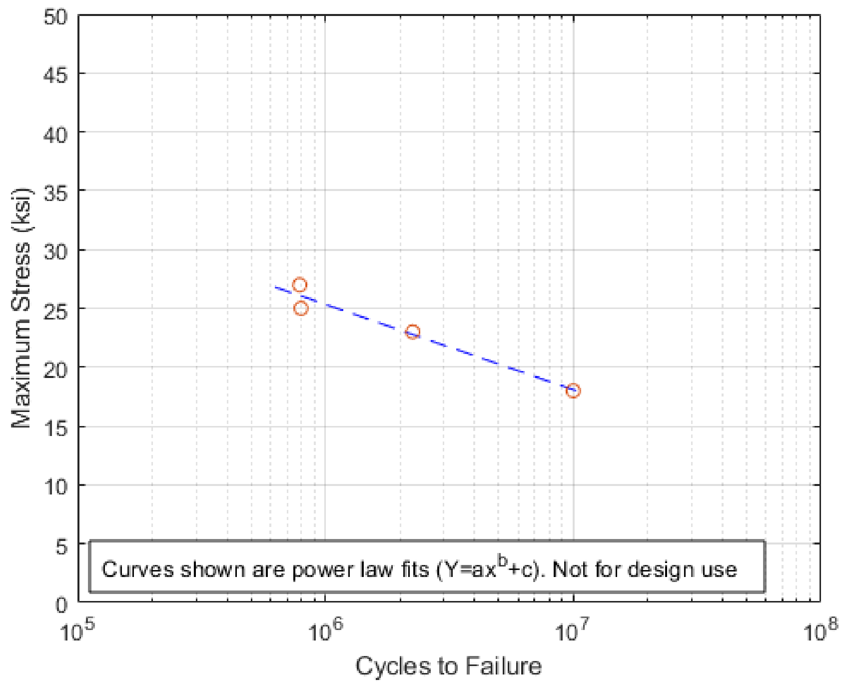

Figure 6. High Cycle Fatigue Results: R=0.1, As-Built Surface, Z Orientation

4. Low Cycle Fatigue

Twenty-two round fatigue specimens were tested in accordance with ASTM E606, *Standard Test Method for Strain-Controlled Fatigue Testing*. The test specimens had a nominal gauge

[3] Gabriel Demeneghi, Baxter Barnes, Paul Gradl, Jason R. Mayeur, Kavan Hazeli, Size Effects on Microstructure and Mechanical Properties of Additively Manufactured Copper-Chromium-Niobium Alloy. Additive Manufacturing 820 (2021), 141511.

[4] Ashley Roach, Benjamin White, Anthony Garland, Jared Bradley, Jay Carroll, Brad Boyce, Size-dependent Stochastic Tensile Properties in Additively Manufactured 316L Stainless Steel. Additive Manufacturing 32 (2020), 101090

diameter of 0.250 inch and a nominal reduced section length of 0.500 inch. Sixteen specimens were tested in lab air at room temperature (approximately 70° F), three specimens were tested at an elevated temperature of 752° F, and three specimens were tested at an elevated temperature of 1112° F. Nineteen specimens were tested in the machined surface condition while three specimens were tested in the as-built surface condition to evaluate the role of surface roughness on fatigue life.

Strain measurements at room temperature were derived from a 0.3 inch extensometer calibrated to ±6% strain. The tests consisted of cyclic loading in strain control using a triangular waveform at 0.5 Hz (for 20 tests) or 0.25 Hz (for 2 tests). The stress ratio (R) was –1 for all tests. The tests were run until the peak cyclic load decreased by 50% from the peak load of a reference cycle or until the specimen fractured, whichever came first. Reference cycles were chosen to be a cycle near the beginning of the test where the strain endpoints had been reached.

Table 6 lists the test results. Strain values are given in total strain, which represents the range of the maximum and minimum applied strain. For example, a test conducted to 1.0% total strain loaded the specimen to +0.5% and –0.5% strain.

Table 6. LCF Results

Specimen	Orientation	Surface Process	Temperature (°F)	Total Strain (%)	Cycles to 50% Load Drop
LM-1-1	Z	Polished	70	0.70	6521
LM-1-2*	Z	Polished	70	0.70	7583
LM-1-3	Z	Polished	70	1.35	980
LM-1-4	Z	Polished	70	0.70	8250
LM-1-5	Z	Polished	70	2.00	392
LM-2-1	Z	Polished	70	1.35	1028
LM-2-2	Z	Polished	70	0.70	7905
LM-2-3	Z	Polished	70	1.35	818
LM-2-4	Z	Polished	70	0.70	6140
LM-2-5	Z	Polished	70	2.00	374
LM-3-1	Z	Polished	752	0.70	3627
LM-3-4	Z	Polished	752	1.35	799
LM-3-5	Z	Polished	752	2.00	473
LM-4-1	Z	Polished	1112	0.70	3491
LM-4-2	Z	Polished	1112	1.35	632
LM-4-3	Z	Polished	1112	2.00	237
LCF-AB-1	Z	As-built	70	0.70	7972
LCF-AB-2	Z	As-built	70	1.35	1111
LCF-AB-3	Z	As-built	70	2.00	469
LCF-XY-1	XY	Polished	70	0.70	4495
LCF-XY-2	XY	Polished	70	1.35	856
LCF-XY-3	XY	Polished	70	2.00	381

*Stress ratio was not exactly R=-1 for this test. Cycles to 50% Load Drop is still in family with similar specimens

Strain-life curves are shown for 70° F, 752° F, and 1112° F polished Z-oriented specimens (Figure 7), 70° F as-built Z-oriented specimens (Figure 8), and 70° F polished XY-oriented specimens (Figure 9).

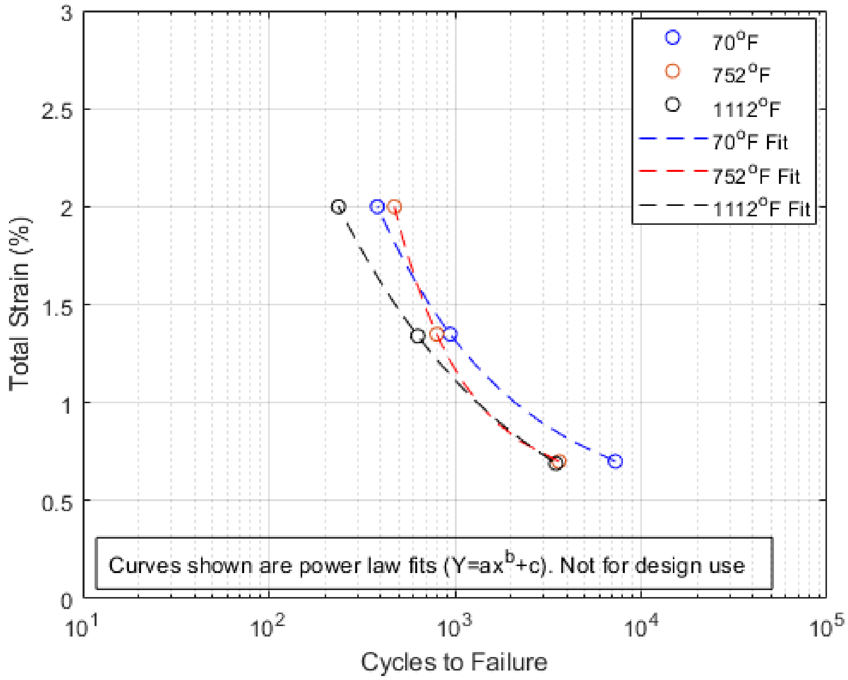

Figure 7. LCF Results: R = -1, Low Stress Ground & Polished, Z Orientation, 70°, 752˚, and 1112˚ F

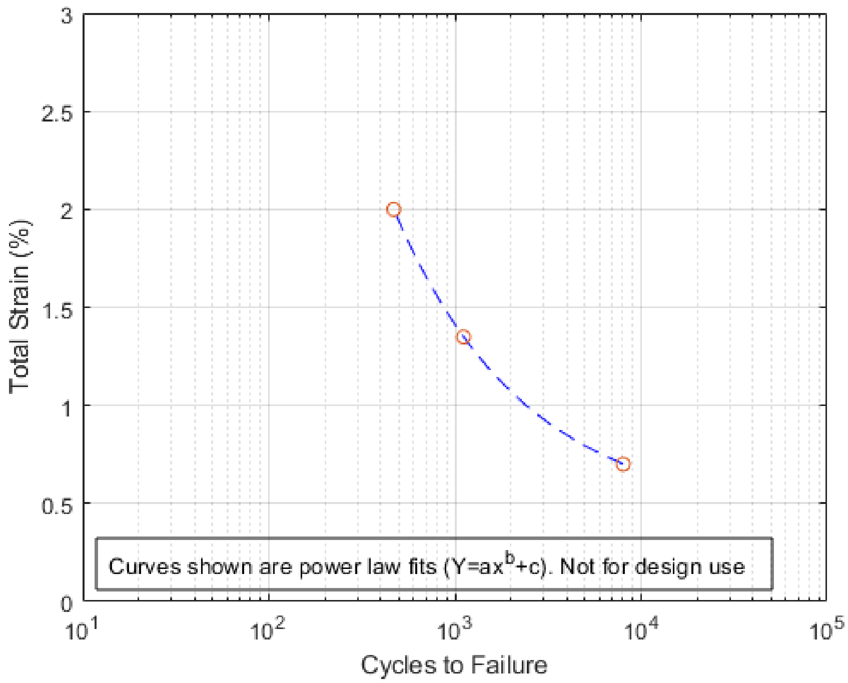

Figure 8. LCF Results: R = -1, As-Built Surface, Z Orientation, 70°F

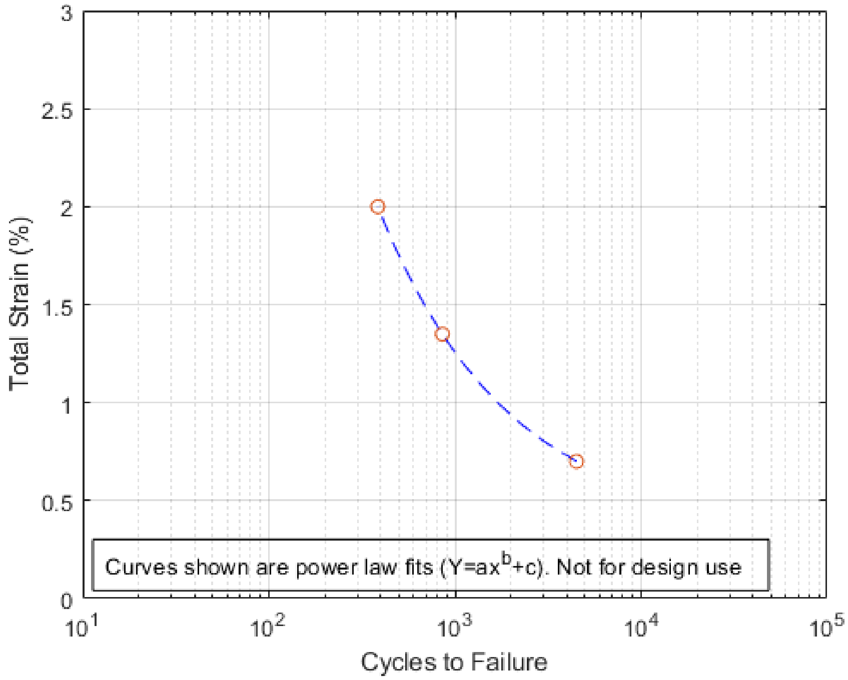

Figure 9. LCF Results: R = -1, Low Stress Ground & Polished, XY Orientation, 70°F

5. Fracture Toughness

Three compact tension specimens of additively manufactured GRCop-42 were tested in accordance with ASTM E1820, *Standard Test Method for Measurement of Fracture Toughness.* Test specimens were fabricated per S-318 Rev A with W = 2.00 inches and B = 1.00 inch. The environment for this testing was lab air at room temperature, approximately 70˚ F. The specimens were precracked and tested on Test Station 2 in Building 4602 at MSFC. Results for test specimen FT-1 are not included in this report because the specimen failed to generate any valid data points during testing. The results from FT-1 were used to adjust testing parameters on FT-2 and FT-3 to generate tests containing valid data points.

Table 6. Fracture Toughness Properties (ASTM E1820)

Samples	J_q (in-lbs/in^2)	K_{iq} (ksi√in)	Validity	Engineering Judgement
FT-2	365.6	104.66	Not Valid	Useful
FT-3	595.5	132.66	Not Valid	Likely not useful

Detailed test results from which to draw conclusions on the usefulness of the invalid tests are included in Appendix 4.

6. Fatigue Crack Growth Rate

Four compact tension specimens of additively manufactured GRCop-42 were tested in accordance with ASTM E647, *Standard Test Method for Fatigue Crack Growth Rates*. Test specimens were fabricated per S-333 Rev C with W = 1.50 inches and B = 0.375 inch. The environment for this testing was lab air at room temperature, approximately 70˚ F. Two additional specimens (Fracture-1 and Fracture-2) with W = 3.0 inches and B = 0.75 inches were tested in an attempt to obtain adequate Region 2 and Region 3 results.

Table 7 lists the tested FCGR specimens along with the initial applied K_{max} and the loading ratio. Specimens Crack-Growth-1, Crack-Growth-2, Fracture-1, and Fracture-2 were tested in increasing K control, while specimens Crack-Growth-3 and Crack-Growth-6 were tested in decreasing K control. Crack-Growth-1, Crack-Growth-2, Crack-Growth-6, Fracture-1, and Fracture-2 were tested in Fixed R mode. Crack-Growth-3 was tested in Constant K_{max} mode. Due to the high strain hardening properties of GRCop-42, flow strength was used in place of yield strength during testing for specimens Crack-Growth-1, Crack-Growth-2, Fracture-1, and Fracture-2 based on guidance in ASTM E647, Section 7.2.1. Specimen Crack-Growth-6 was used for two threshold tests at R=0.1 and R=0.7. Figure 10 shows a plot of the test data. The data points from each test are tabulated in Appendix 5.

Table 7. Fatigue Crack Growth Rate Test Parameters

Sample	Initial K_{max}	Initial Load Ratio
Crack-Growth-1	7.7	0.10
Crack-Growth-2	14.1	0.70
Crack-Growth-3	16.3	0.10
Crack-Growth-6 T1	8.2	0.10
Crack-Growth-6 T2	6.1	0.70
Fracture-1	14.9	0.10
Fracture-2	22.3	0.70

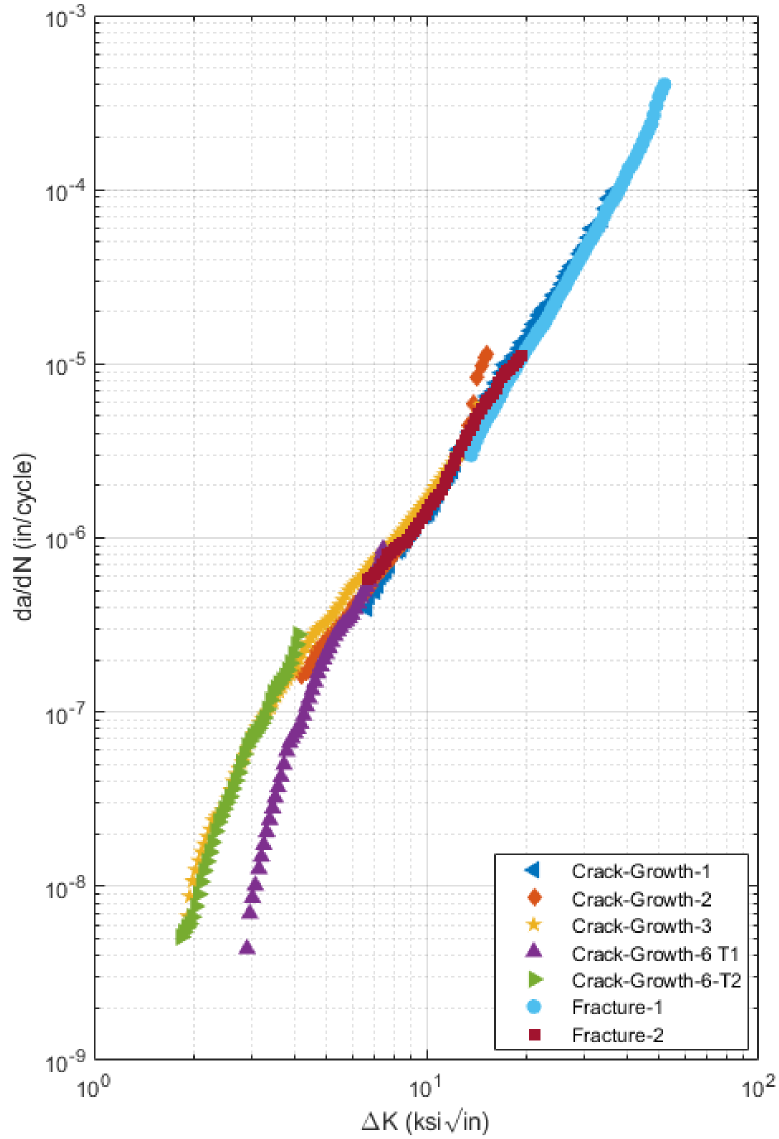

Figure 10. FCGR Test Results

Registration – Material Properties Suite
Material Property Suite: N/A
Please see NASA-STD-6030 for guidance and requirements for registration of a material process to an MPS.

Appendix 1. Unauthorized Build Restart Details

Build -0230 (QMP Build 1)

This build was stopped and restarted six times, totaling approximately 6.5 days, as follows:

1. Layer 1169 for approximately 22 hours
2. Layer 1269 for approximately 22 hours
3. Layer 1282 for approximately 22 hours
4. Layer 2281 for approximately 89 hours
5. Layer 2292 for approximately 40 seconds
6. Layer 3287 for approximately 1.5 hours

Build -0276 (Thin Section)

This build was stopped and restarted once, totaling approximately 4 minutes, as follows:

1. Layer 994 for approximately 4 minutes

Build -0392 (QMP Build 5)

This build was stopped and restarted once, totaling approximately 1 minute, as follows:

2. Layer 4 for approximately 1 minute

Build -0393 (QMP Build 6)

This build was stopped and restarted once, totaling approximately 3 minutes, as follows:

1. Layer 1 for approximately 3 minutes

Build -0406 (QMP Build 7)

This build was stopped and restarted twice, totaling approximately 12.5 hours, as follows:

1. Layer 5 for approximately 1 minute
2. Layer 1375 for approximately 12.5 hours

Appendix 2. Individual Tensile Test Results

Specimen	Orient.	Surface Process	Temperature (°F)	Ult. Tensile Stress (ksi)	Yld Stress (ksi)	Elongation (%)
TM1-1	Z	Machined	70	53.82	28.64	31.05
TM1-2	Z	Machined	70	53.19	27.94	30.94
TM1-3	Z	Machined	70	53.45	27.94	31.11
TM2-1	Z	Machined	70	53.21	27.86	31.46
TM2-2	Z	Machined	70	53.29	27.80	31.39
TM2-3	Z	Machined	70	53.24	27.92	31.39
TM4-1	Z	Machined	70	53.11	27.68	30.94
TM4-2	Z	Machined	70	52.84	27.54	31.21
TM4-3	Z	Machined	70	53.39	28.12	30.87
TM4-4	Z	Machined	70	53.23	28.06	31.34
WT-1*	Z	Machined	70	46.01	27.85	4.57
WT-2	Z	Machined	70	53.55	28.24	27.15
WT-3	Z	Machined	70	53.86	28.08	26.12
WT-4	Z	Machined	70	53.86	28.89	25.54
WT-5	Z	Machined	70	53.59	28.34	26.64
WT-6	Z	Machined	70	54.15	28.86	26.58
TEN-AB-1	Z	As-built	70	49.17	25.11	28.47
TEN-AB-2	Z	As-built	70	49.11	25.04	29.74
TEN-AB-3	Z	As-built	70	48.95	25.28	33.73
0392-Witness-1	Z	Machined	70	53.51	28.26	29.58
0392-Witness-2	Z	Machined	70	53.84	28.61	29.96
0392-Witness-3	Z	Machined	70	53.42	28.20	28.96
0392-Witness-4	Z	Machined	70	53.96	27.94	29.65
0392-Witness-5	Z	Machined	70	54.02	28.60	29.63
0392-Witness-6	Z	Machined	70	53.87	28.49	29.31
0393-Witness-1	Z	Machined	70	54.73	29.32	29.46
0393-Witness-2	Z	Machined	70	54.80	29.41	29.08
0393-Witness-3	Z	Machined	70	54.49	29.13	29.23
0393-Witness-4	Z	Machined	70	54.55	29.12	29.72
0393-Witness-5	Z	Machined	70	55.25	29.26	29.27
0393-Witness-6	Z	Machined	70	54.66	29.37	29.52
TEN-XY-1	XY	Machined	70	56.47	30.86	29.35
TEN-XY-2	XY	Machined	70	56.29	31.02	29.34
TEN-XY-3	XY	Machined	70	56.33	30.91	29.48
TM-6-1	Z	Machined	750	27.94	21.79	22.15
TM-6-3	Z	Machined	750	27.98	21.63	21.32
TM-6-2	Z	Machined	750	28.22	21.76	21.76
TM-7-1	Z	Machined	1112	18.24	16.75	42.19
TM-7-2	Z	Machined	1112	18.07	16.79	39.78
TM-7-3	Z	Machined	1112	17.78	16.70	37.56

*One machined-finished Z-direction specimen in the present study (specimen WT-1) fractured at 46.01 ksi with an elongation of 4.57% (14% lower than average tensile strength and 85% lower than average elongation). Production of this specimen was potentially interrupted by an unplanned build restart. A much flatter fracture surface was observed for this specimen compared to typical specimens in this study. When examined under partial ring lighting, scan line texturing was observed, suggesting there may have been defects in the fracture region contributing to the premature failure. Figure 11 demonstrates the difference in the fracture surfaces between the prematurely failed specimen (WT-1) and a typical specimen (WT-2).

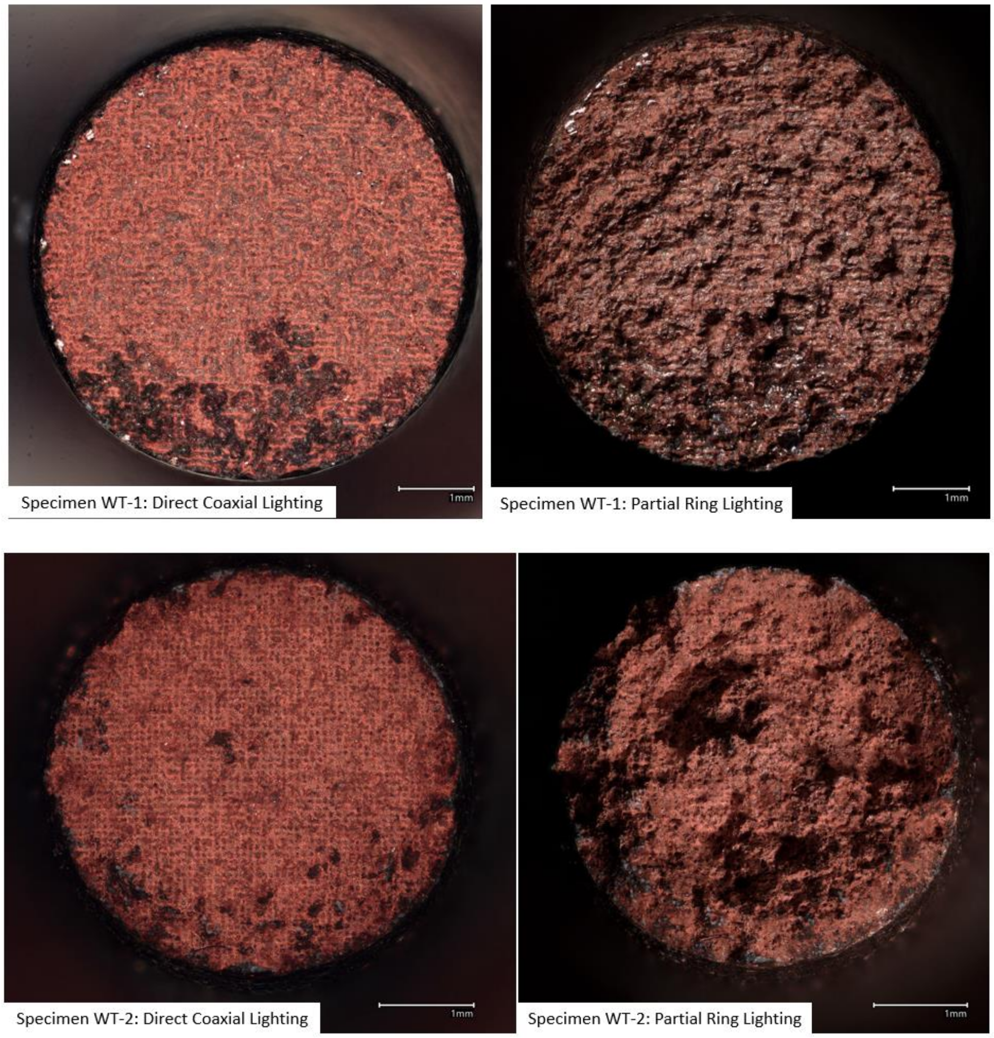

Figure 11. Visible differences in fracture surface between prematurely-failed specimen WT-1 and typical specimen WT-2.

Appendix 3. Individual Thin-Wall Tensile Test Results

Specimen	Thickness (in)	Ult. Tensile Stress (ksi)	Yld. Stress (ksi)	Elongation (%)
B1	0.25	47.50	24.61	30.23
B2	0.20	47.20	25.11	29.82
B3	0.06	39.79	21.52	20.30
B4	0.08	41.78	21.70	23.31
B5	0.04	34.19	18.82	18.49
B6	0.03	30.47	16.16	15.81
B7	0.05	37.47	19.89	21.12
B8	0.10	43.67	23.19	25.16
B9	0.25	47.56	25.26	30.84
C1	0.25	47.51	24.84	30.59
C2	0.20	46.77	23.74	28.43
C3	0.06	39.55	20.58	18.72

C4	0.08	42.15	22.63	23.10
C5	0.04	33.95	18.86	16.85
C6	0.03	30.04	16.79	10.04
C7	0.05	38.27	20.61	19.64
C8	0.10	43.80	24.10	22.85
C9	0.25	47.66	25.39	29.17
D1	0.25	48.02	24.73	26.76
D2	0.20	46.98	23.94	24.60
D3	0.06	39.71	21.78	17.50
D4	0.08	41.83	22.49	18.43
D5	0.04	34.41	19.00	11.89
D6	0.03	29.88	16.72	8.38
D7	0.05	37.52	20.40	16.12
D8	0.10	43.14	22.29	19.38
D9	0.25	47.06	24.62	28.01
E1	0.25	47.61	24.51	27.69
E2	0.20	46.82	24.50	26.81
E3	0.06	39.04	20.61	20.24
E4	0.08	41.50	22.17	22.40
E5	0.04	34.01	18.04	15.99
E6	0.03	30.11	16.26	13.03
E7	0.05	37.29	20.36	19.19
E8	0.10	42.94	21.89	23.52
E9	0.25	47.48	24.52	30.06
F1	0.25	47.43	25.15	30.11
F2	0.20	46.12	23.89	28.43
F3	0.06	39.45	20.37	21.50
F4	0.08	41.90	22.34	23.93
F5	0.04	34.09	19.14	17.55
F6	0.03	29.64	16.05	15.09
F7	0.05	37.83	20.03	21.37
F8	0.10	43.11	21.17	24.07
F9	0.25	47.42	24.53	29.48
G1	0.25	47.74	24.79	27.92
G2	0.20	46.67	22.98	21.89
G3	0.06	38.77	19.94	15.66
G4	0.08	41.52	21.21	17.04
G5	0.04	30.96	18.18	6.12
G6	0.03	25.44	15.70	4.29
G7	0.05	37.12	19.83	13.48
G8	0.10	43.47	22.26	17.77
G9	0.25	47.33	24.50	24.75
H1	0.25	47.46	24.52	28.57
H2	0.20	46.61	25.06	26.65
H3	0.06	39.50	21.07	20.37
H4	0.08	41.28	21.87	21.17
H5	0.04	33.86	18.59	17.32
H6	0.03	30.15	15.93	13.28
H7	0.05	37.58	21.07	17.02
H8	0.10	43.31	22.66	24.52
H9	0.25	47.64	24.95	26.89

Appendix 4. Fracture Toughness Test Results

GRCop42 QMP Build 6, Work Order #2021-0393, Sequence 8 Test Report

Appendix 5. Fatigue Crack Growth Rate Data

Crack-Growth-1 (R=0.1)		Crack-Growth-2 (R=0.7)		Crack-Growth-3 (R=0.1)		Crack-Growth-6 T1 (R=0.1)		Crack-Growth-6 T2 (R=0.7)	
da/dN (in/cycle)	**Delta K (ksi√(in))**	**da/dN (in/cycle)**	**Delta K (ksi√(in))**	**da/dN (in/cycle)**	**Delta K (ksi√(in))**	**da/dN (in/cycle)**	**Delta K (ksi√(in))**	**da/dN (in/cycle)**	**Delta K (ksi√(in))**
3.94E-07	6.62819	1.63E-07	4.2295643	5.88E-06	14.653065	8.05E-07	7.365710017	2.79E-07	4.120384769
4.62E-07	6.74403	1.71E-07	4.3394148	5.70E-06	14.579999	8.64E-07	7.418369763	2.44E-07	4.063953521
5.01E-07	6.88043	1.95E-07	4.5154158	5.08E-06	14.404663	8.27E-07	7.454202817	2.15E-07	3.98684989
4.94E-07	7.01996	2.28E-07	4.6933418	4.44E-06	14.116202	7.89E-07	7.410541867	1.91E-07	3.900833206
5.37E-07	7.15953	2.47E-07	4.8651371	4.03E-06	13.818622	7.48E-07	7.310378237	1.74E-07	3.824032904
5.97E-07	7.29985	2.71E-07	5.0632116	3.71E-06	13.524117	7.03E-07	7.166720094	1.61E-07	3.749027559
6.26E-07	7.44607	2.85E-07	5.2432523	3.49E-06	13.251222	6.57E-07	7.014980939	1.53E-07	3.673370643
6.48E-07	7.59695	3.12E-07	5.4341165	3.33E-06	12.979567	6.09E-07	6.876820523	1.45E-07	3.599464202
6.94E-07	7.7466	3.40E-07	5.6599841	3.17E-06	12.726967	5.64E-07	6.743691709	1.37E-07	3.528673933
8.18E-07	7.89956	3.76E-07	5.8500194	3.01E-06	12.48247	5.26E-07	6.612866027	1.29E-07	3.458918042
8.92E-07	8.06235	4.13E-07	6.060544	2.85E-06	12.234238	4.90E-07	6.482738707	1.17E-07	3.393232726
8.42E-07	8.22539	4.36E-07	6.2524925	2.71E-06	11.987946	4.55E-07	6.354069829	1.04E-07	3.324690815
8.59E-07	8.38599	4.65E-07	6.4421509	2.57E-06	11.743362	4.22E-07	6.231559493	9.30E-08	3.256400577
9.25E-07	8.55366	4.89E-07	6.606226	2.44E-06	11.514782	3.91E-07	6.107005945	8.63E-08	3.196090325
1.00E-06	8.72977	5.32E-07	6.7984286	2.32E-06	11.288358	3.64E-07	5.983572585	8.09E-08	3.133475247
1.06E-06	8.90786	5.79E-07	6.999077	2.20E-06	11.061039	3.46E-07	5.870656284	7.65E-08	3.071068959
1.11E-06	9.08481	6.22E-07	7.169287	2.08E-06	10.839587	3.33E-07	5.757120327	7.27E-08	3.011257256
1.15E-06	9.2669	6.63E-07	7.360997	1.96E-06	10.622915	3.22E-07	5.640622308	6.84E-08	2.949287401
1.26E-06	9.45342	7.03E-07	7.5767608	1.85E-06	10.415356	3.06E-07	5.526885392	6.38E-08	2.891344646
1.37E-06	9.64561	7.48E-07	7.7857512	1.75E-06	10.206185	2.92E-07	5.423745454	5.74E-08	2.836873186
1.34E-06	9.84073	8.09E-07	8.0138736	1.66E-06	10.005102	2.75E-07	5.318104255	5.10E-08	2.777782701
1.36E-06	10.03216	8.73E-07	8.248332	1.58E-06	9.8093079	2.53E-07	5.206456747	4.51E-08	2.723086773
1.39E-06	10.22648	9.24E-07	8.4626165	1.51E-06	9.6137429	2.33E-07	5.105784712	4.04E-08	2.670598374
1.49E-06	10.43418	9.90E-07	8.6713589	1.44E-06	9.4211686	2.16E-07	5.009180094	3.63E-08	2.615837706
1.58E-06	10.64881	1.06E-06	8.9116875	1.37E-06	9.234678	2.01E-07	4.913185976	3.28E-08	2.564893429
1.77E-06	10.86417	1.14E-06	9.1725329	1.30E-06	9.0551047	1.84E-07	4.817979127	3.03E-08	2.514662301
2.01E-06	11.08639	1.24E-06	9.4321909	1.24E-06	8.8712218	1.67E-07	4.722524255	2.78E-08	2.460850902
2.10E-06	11.30776	1.36E-06	9.6970629	1.18E-06	8.6925847	1.49E-07	4.628592982	2.54E-08	2.41486563
2.24E-06	11.53184	1.48E-06	9.967613	1.12E-06	8.5244071	1.34E-07	4.535009893	2.34E-08	2.37197367

2.30E-06	11.76857	1.62E-06	10.230186	1.07E-06	8.3552272	1.20E-07	4.444774632	2.07E-08	2.321091838
2.42E-06	12.00682	1.77E-06	10.513899	1.02E-06	8.1862627	1.08E-07	4.361640563	1.79E-08	2.274752615
2.66E-06	12.24248	1.91E-06	10.802186	9.75E-07	8.0223177	9.58E-08	4.278222325	1.57E-08	2.231143308
3.20E-06	12.49028	2.06E-06	11.08076	9.32E-07	7.8610486	8.57E-08	4.196047661	1.39E-08	2.186154092
3.13E-06	12.74237	2.23E-06	11.396383	8.90E-07	7.7025923	8.00E-08	4.114386266	1.23E-08	2.144283445
3.42E-06	12.99873	2.41E-06	11.71001	8.56E-07	7.5607265	7.58E-08	4.027507167	1.06E-08	2.102314368
3.60E-06	13.26333	2.61E-06	12.04434	8.23E-07	7.4137194	7.10E-08	3.951507743	8.99E-09	2.061564468
4.09E-06	13.52984	2.87E-06	12.406382	7.95E-07	7.2594973	6.68E-08	3.883442483	7.66E-09	2.020703101
4.45E-06	13.80645	3.17E-06	12.734148	7.68E-07	7.115172	5.96E-08	3.806869155	6.66E-09	1.976379741
4.74E-06	14.08679	3.65E-06	13.078828	7.43E-07	6.9762636	5.00E-08	3.73032409	6.09E-09	1.937122447
5.04E-06	14.36852	4.45E-06	13.449598	7.15E-07	6.838968	4.25E-08	3.659786465	5.79E-09	1.901051014
5.25E-06	14.65179	5.89E-06	13.840995	6.77E-07	6.7023193	3.71E-08	3.585052992	5.44E-09	1.86272475
6.03E-06	14.94154	8.43E-06	14.258998	6.42E-07	6.5732461	3.23E-08	3.511819347	5.11E-09	1.82901291
6.50E-06	15.24647	9.76E-06	14.661881	6.09E-07	6.4460641	2.80E-08	3.449592141		
6.43E-06	15.55786	1.08E-05	15.001456	5.82E-07	6.314012	2.41E-08	3.379777311		
6.99E-06	15.87543	1.14E-05	15.232438	5.64E-07	6.1880253	2.05E-08	3.309943159		
7.75E-06	16.2047			5.44E-07	6.0655862	1.73E-08	3.243742271		
7.85E-06	16.52842			5.23E-07	5.9431728	1.48E-08	3.191887936		
8.87E-06	16.85166			4.99E-07	5.8300243	1.26E-08	3.136127718		
9.88E-06	17.1985			4.71E-07	5.7156871	1.01E-08	3.061355889		
9.55E-06	17.54876			4.40E-07	5.6011652	8.58E-09	2.998672061		
1.00E-05	17.89433			4.12E-07	5.4875927	6.96E-09	2.945565301		
1.10E-05	18.25928			3.91E-07	5.376461	4.37E-09	2.888683152		
1.13E-05	18.63878			3.70E-07	5.2701323				
1.22E-05	19.01459			3.52E-07	5.1698215				
1.32E-05	19.38802			3.37E-07	5.0699209				
1.35E-05	19.78213			3.25E-07	4.9653912				
1.42E-05	20.19801			3.15E-07	4.8632882				
1.55E-05	20.60953			3.05E-07	4.7717258				
1.68E-05	21.02011			2.95E-07	4.6798803				
1.74E-05	21.4379			2.80E-07	4.5866731				
1.90E-05	21.8671			2.65E-07	4.4952999				
2.02E-05	22.30783			2.49E-07	4.4065011				
2.10E-05	22.76542			2.34E-07	4.3202197				
2.21E-05	23.23061			2.18E-07	4.2362453				
2.26E-05	23.68805			2.01E-07	4.1495832				

2.47E-05	24.17142		1.86E-07	4.0662605		
2.38E-05	24.66588		1.74E-07	3.9887983		
2.66E-05	25.16487		1.64E-07	3.9095038		
2.87E-05	25.66736		1.55E-07	3.8305519		
3.16E-05	26.16248		1.47E-07	3.7557861		
3.38E-05	26.69129		1.39E-07	3.6830835		
3.62E-05	27.25534		1.31E-07	3.610502		
3.74E-05	27.81352		1.23E-07	3.5393557		
3.88E-05	28.35784		1.14E-07	3.4677243		
4.28E-05	28.91654		1.06E-07	3.3983957		
4.51E-05	29.51583		1.01E-07	3.3336624		
4.76E-05	30.13745		9.60E-08	3.267252		
5.30E-05	30.74294		9.18E-08	3.2013633		
5.97E-05	31.36032		8.71E-08	3.1401075		
6.08E-05	31.9998		8.16E-08	3.0780721		
6.24E-05	32.63322		7.47E-08	3.0155111		
6.42E-05	33.27023		6.82E-08	2.9577544		
6.72E-05	33.92698		6.22E-08	2.9015495		
7.78E-05	34.60423		5.63E-08	2.8421357		
8.84E-05	35.31833		5.15E-08	2.7838212		
9.16E-05	36.05787		4.75E-08	2.7297939		
9.77E-05	36.80293		4.40E-08	2.6765664		
9.92E-05	37.54889		4.01E-08	2.6233739		
			3.57E-08	2.5716852		
			3.20E-08	2.5254345		
			2.90E-08	2.4765079		
			2.73E-08	2.4227295		
			2.60E-08	2.3747363		
			2.50E-08	2.3320586		
			2.39E-08	2.283085		
			2.12E-08	2.2361082		
			1.92E-08	2.1930542		
			1.74E-08	2.1499921		
			1.57E-08	2.1078707		
			1.40E-08	2.0670252		
			1.24E-08	2.0250727		

				1.07E-08	1.9838189				
				8.75E-09	1.9435004				
				6.72E-09	1.912873				

Fracture-1 (R=0.1)		**Fracture-2 (R=0.7)**	
da/dN (in/cycle)	**Delta K (ksi√(in))**	**da/dN (in/cycle)**	**Delta K (ksi√(in))**
3.46E-06	13.38896	5.79E-07	6.684808
3E-06	13.6291	5.86E-07	6.816583
3.32E-06	13.89029	6.11E-07	6.949528
3.66E-06	14.16065	6.25E-07	7.079374
3.99E-06	14.44212	6.63E-07	7.232399
4.25E-06	14.71037	7.04E-07	7.379791
4.57E-06	14.98415	7.43E-07	7.5143
4.88E-06	15.28014	7.97E-07	7.665661
5.15E-06	15.58213	8.28E-07	7.818418
5.49E-06	15.892	8.54E-07	7.973364
5.86E-06	16.17948	8.79E-07	8.125112
6.32E-06	16.48889	9.11E-07	8.28957
6.78E-06	16.82585	9.29E-07	8.463026
7.31E-06	17.14341	9.41E-07	8.618643
7.83E-06	17.45972	9.88E-07	8.78945
8.29E-06	17.80989	1.05E-06	8.978319
8.76E-06	18.14657	1.09E-06	9.151999
9.28E-06	18.49418	1.15E-06	9.315838
9.99E-06	18.87001	1.23E-06	9.509816
1.07E-05	19.24051	1.29E-06	9.721283
1.13E-05	19.60697	1.37E-06	9.905987
1.2E-05	19.96587	1.46E-06	10.09733
1.27E-05	20.37182	1.56E-06	10.30108
1.35E-05	20.76639	1.62E-06	10.4949
1.42E-05	21.13914	1.71E-06	10.70191
1.51E-05	21.57285	1.79E-06	10.92192
1.59E-05	22.00335	1.89E-06	11.14762
1.67E-05	22.40739	2.05E-06	11.37116
1.76E-05	22.84429	2.24E-06	11.5908
1.89E-05	23.30657	2.43E-06	11.82008
2.03E-05	23.76823	2.63E-06	12.03387
2.18E-05	24.22994	2.86E-06	12.27882
2.33E-05	24.67296	3.15E-06	12.54738
2.48E-05	25.12601	3.44E-06	12.79115
2.63E-05	25.63527	3.68E-06	13.02482
2.8E-05	26.15622	3.92E-06	13.27954

3E-05	26.67027	4.16E-06	13.56124
3.22E-05	27.18028	4.45E-06	13.83481
3.42E-05	27.7042	4.8E-06	14.09948
3.66E-05	28.23464	5.14E-06	14.38158
3.91E-05	28.78567	5.53E-06	14.66241
4.16E-05	29.35081	5.9E-06	14.95246
4.44E-05	29.90102	6.19E-06	15.27209
4.78E-05	30.47397	6.39E-06	15.55599
5.09E-05	31.08101	6.69E-06	15.84228
5.37E-05	31.65304	7.24E-06	16.18498
5.72E-05	32.26601	7.8E-06	16.51021
6.1E-05	32.9135	8.29E-06	16.82125
6.54E-05	33.57135	8.73E-06	17.1525
7.08E-05	34.24151	9.1E-06	17.50748
7.68E-05	34.91225	9.35E-06	17.85264
8.23E-05	35.60439	9.74E-06	18.20882
8.64E-05	36.28522	1.02E-05	18.59762
9.05E-05	36.93303	1.06E-05	18.94097
9.64E-05	37.59426	1.1E-05	19.27786
0.000104	38.37145		
0.000112	39.15665		
0.000122	39.89905		
0.000133	40.66527		
0.000139	41.50246		
0.000147	42.22299		
0.000159	43.01218		
0.000172	43.90827		
0.000187	44.82327		
0.000205	45.72282		
0.00022	46.58118		
0.000239	47.43434		
0.000267	48.26516		
0.000304	49.14749		
0.000342	50.15198		
0.000371	51.03336		
0.000401	51.99735		